Alice ITS Upgrade

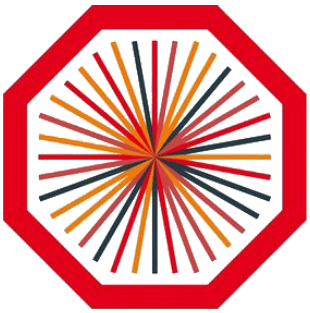

Readout Electronic – WP10

Last revision – 06 January 2016

Major changes

20 Dec 2015

- Cables data updated.

05 Jan 2016

- General review and expansion.
- Update simulations section (merged from separate simulation note).
- Updated radiation levels (latest values as Dec 2015).
- Added section on radiation hardness design/testing.

05 Jan 2016

- Added section on data routing between sensor and optical links.
- Added section on trigger connection and timing.

0 Contents

1 System overview

1.1 Sensors layout and interconnections

The ITS is divided into three main region, Inner (3 layers), Middle (2 layers) and Outer (2 layers), each characterized by a different mechanical arrangement of the sensors around the beam axis. From the readout electronic point of view, what relevant is the different operating mode of the sensors in such regions and the different speed of the data streams, which depends on the physics implementation of the data bus.

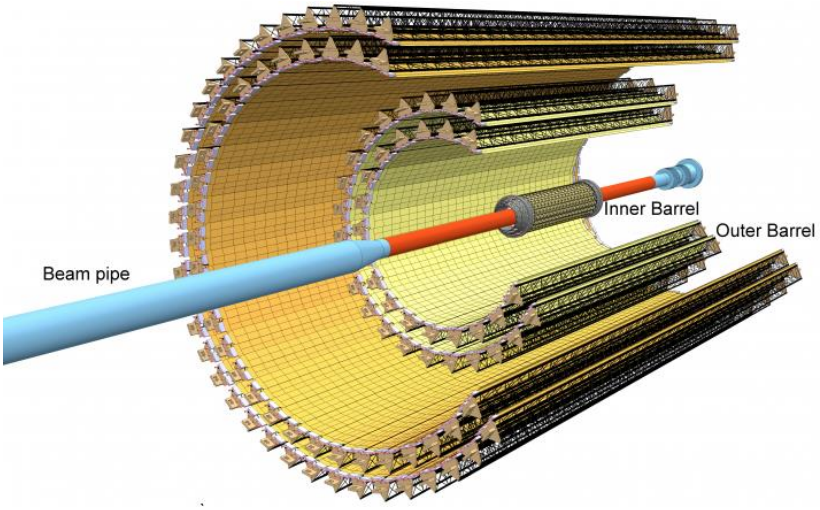

Figure 1 – ALICE Inner Tracking System seven layers layout, with the two Outer and two Middle layers clearly visible, and the three Inner layers closer to the beam pipe.

1.1.1 Inner Layers

The three innermost layers are composed by a different number of identical staves, each one supporting nine chips. Each chip has dedicated bus lines to receive and send data from/to the Readout Electronics.

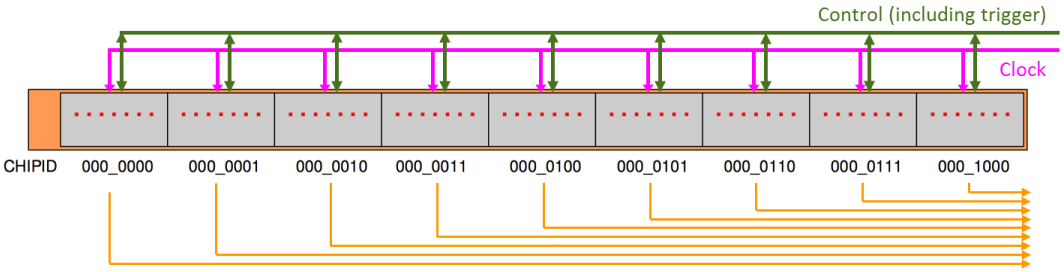

Figure 2 – inner Layers stave sensors and connections schematic.

Figure 2 illustrates all the links connecting the sensors with the readout electronics. The clock link (purple) is a mono-directional, multi-drop differential connection running at 40 MHz. The control link (green) is a bi-directional multi-drop differential connection mastered by the Readout Electronics, which can run up to 40 Mb/s. The control link will also carry the trigger, as a special, high priority packet [protocols, control section]. During acquisition time the control line will just carry the trigger and some slow control commands; while not running the detector it will be instead mostly used for reading back sensors status and parameters for setup and control purposes.

Orange lines in Figure 2 represent the high-speed data lines, which are point-to-point, one way differential links connecting each sensor directly to the Readout Electronic.

1.1.2 Middle and Outer Layers

While composed by staves of different lengths, both the Middle and Outer Layers share the same sensing element, the so-called module, and therefore are identical from the readout point of view. A module is composed by two rows of seven sensors, and each row has a master sensor which communicate with the outside world, while the other six chips share a bus to send and receive data to/from the master. The master chip will have a digital interface identical to the Inner Layers chips (in fact it could be the very same chip), therefore the control lines will be identical. With reference to Figure 3, the clock link (purple) is a mono-directional, multi-drop differential connection running at 40 MHz. The control link (green) is a bi-directional multi-drop differential connection mastered by the Readout Electronics, which can run up to 40 Mb/s. The control link will also carry the trigger, as a special, high priority packet [protocols, control section]. During acquisition time the control line will just carry the trigger and some slow control commands, while it will be used for reading back sensors status and parameters for setup and control purposes.

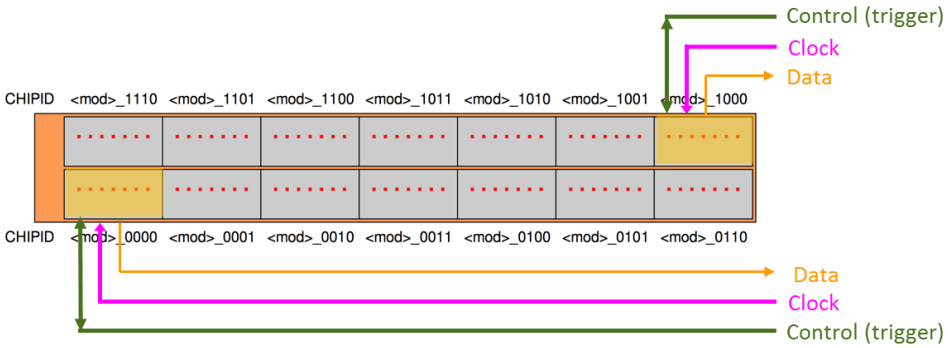

Figure 3 – Module layout with links.

Data lines will be again a point-to-point differential link connected directly to the Readout Electronics. The slave sensors communicate with the master by a dedicated, 4 bit single ended bus connecting the master and the six slaves. The Middle Layers will be composed by staves carrying two rows of four modules each (Figure 4), while the Outer Modules by staves carrying two rows of seven modules each (Figure 5).

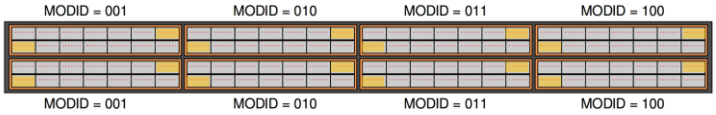

Figure 4 – Middle Layers stave modules arrangement (master sensors in orange).

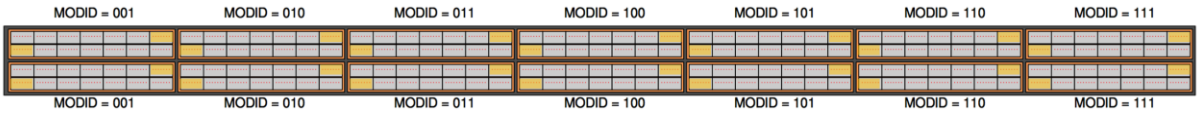

Figure 5 – Outer Layers stave modules arrangement (master sensors in orange).

1.1.3 Links and connections

The topologies illustrated in the previous section requires the signal to and from the sensor to travel through a bus for the full length of the stave, at which end a copper link will connect it to the Readout Electronic in the cavern. Simulations (communication line models) and early prototyping did show how the main limit for high-speed communication comes from the bus, while the copper links (about 4 meter long for all the layers) play a lesser role (but not negligible for the faster inner layers link, see **Error! Reference source ot found.**).

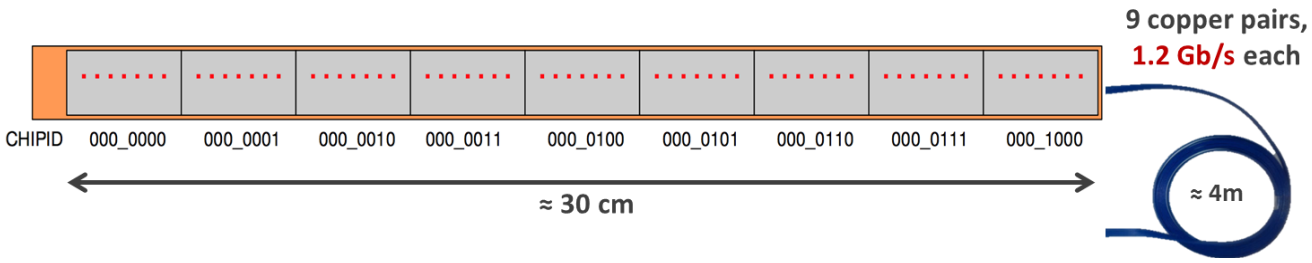

Figure 6 – Inner staves links.

What important for this general system overview, the bandwidth available to transmit the data is limited to 1.2 Gb/s for the Inner Layers link, and to 400 Mb/s for the Middle and Outer Layers link, where the much longer bus is the bottleneck. These results are detailed in section 4.1 and **Error! Reference source not found.**.

Figure 7 – Middle and outer layers links.

Table 1 summarizes the foreseen links per each layer and the total data bandwidth. The rated values are all maximal system design values, not actual average values, which should stay sensibly lower to ensure smooth operations.

Layer	Staves	Links per stave	Links bandwidth	Link payload	Bandwidth per stave	Payload per stave	Bandwidth per layer	Payload per layer
			[Gb/s]	[Gb/s]	[Gb/s]	[Gb/s]	[Gb/s]	[Gb/s]
0	12	9	1.2	.96	10.8	8.64	129.6	103.68
1	16	9	1.2	.96	10.8	8.64	172.8	138.24
2	20	9	1.2	.96	10.8	8.64	216	172.8
3	24	16	0.4	.32	6.4	5.12	153.6	122.88
4	30	16	0.4	.32	6.4	5.12	192	153.6
5	42	28	0.4	.32	11.2	8.96	470.4	376.32
6	48	28	0.4	.32	11.2	8.96	537.6	430.08
Total							1872	1497.6

Table 1 – Copper links count and capacity summary (max design values).

1.2 Readout Electronics

1.2.1 Overview

The Readout Electronics (RE) interfaces the sensors on the staves of the different layers to the readout, control and trigger systems of the ALICE experiment. On the detector side, it collects the high-speed data streams from the sensors and re-organize them to optimize the data transmission through the e-links [##] used by the Common Readout Unit (CRU) [##]. It also manages the control lines which distribute the trigger, the clock and the slow control commands. The Readout Electronic implements also ancillary functions like the power supply lines monitoring to quickly detect and interrupt latch-up states. On the experiment side, the RE feeds the CRU with the ITS data and collects slow control commands and trigger signals.

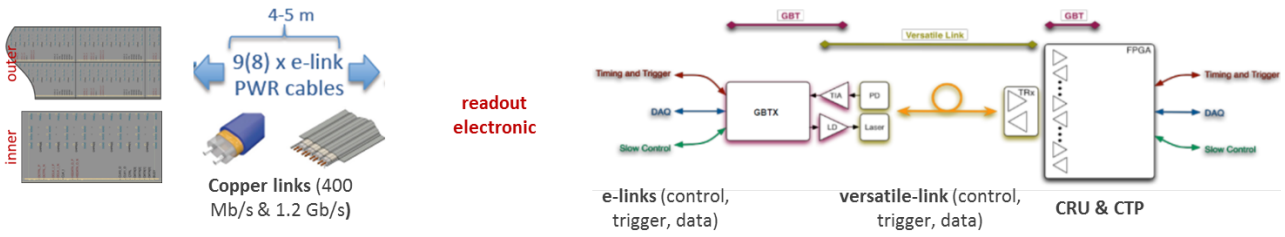

Figure 8 – Readout Electronic main components

Other than signals management and flow control, the Readout Electronics is responsible of managing the following tasks:

- Trigger filtering, i.e. managing triggers to close in time to be successfully accepted by the sensor.
- Busy signal, dealing with sensor/modules not able to handle a trigger.
- Data labelling, to associate data from the sensor with received trigger before sending them to the CRU.
- Monitoring the sensor status by recognizing specific code-word in the data stream.
- Generating the necessary clock/trigger patterns for the sensor, depending which operation mode is selected (continuous/triggered).
- Perform power monitoring, to deal with latch-up states of the sensors.

Figure 9 synthetizes the main functions the Readout Electronic will implement and the data flow to/from the detector and the CRU.

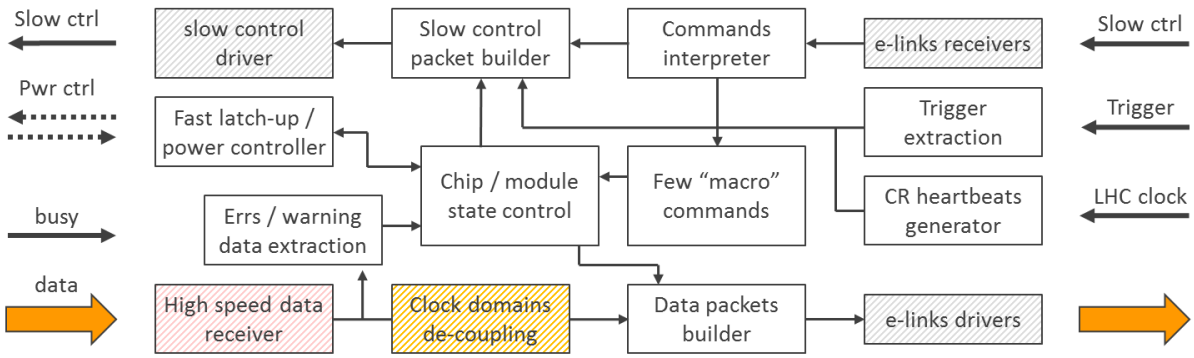

Figure 9 –Readout Electronics main functions.

1.2.2 Readout Units (RUs)

The ITS will be read out and controlled by a cluster of Readout Units (RUs), which will control, trigger and read each single sensor in the detector. The RUs receives control commands and delivers data directly from/to the CRU, via the CERN Versatile Link. To maximize modularity, a single RU design will serve the whole detector, the only difference between RUs attached to different layers being firmware parameters. The

current baseline architecture for the RU is sketched in Figure 10, where only the most important connections are reported.

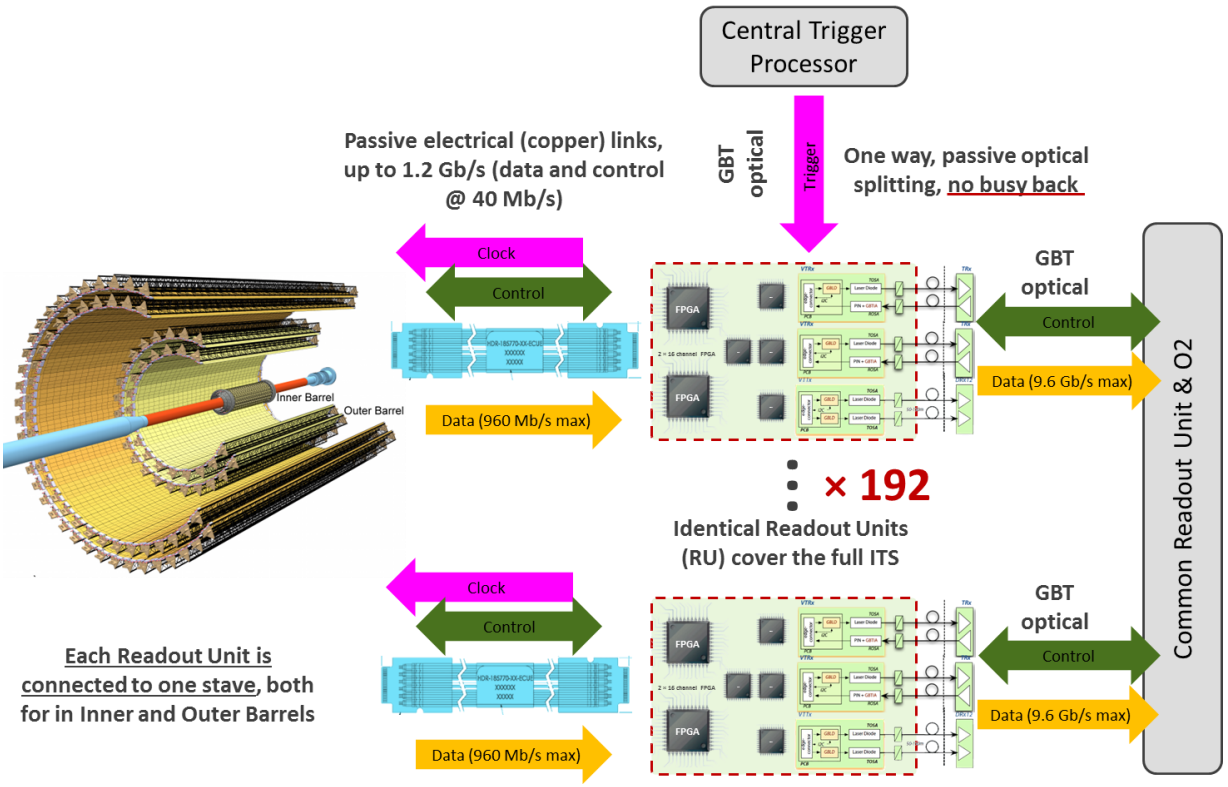

Figure 10 – Readout Unit (RU) modular implementation.

A single RU design able to serve all the layer will host three GBT links paired with one or two main FPGA, each one able to read up to 16 links each from the detector. In the foreseen configuration, in every layer one Readout Unit will read one full stave. This arrangement ensures full modularity and a near-optimal usage of the Versatile Link payload bandwidth (3.2 Gb/s). Table 2 summarize the RUs and GBTx chipsets necessary to read out the entire ITS.

Readout Units and GBT links for maximum design rates

Layer	Staves	Copper assemblies	Copper capacity	RUs per stave	RUs per layer	VTRx count	VTTx count	Data fibers	Control fibers	Data fibers capacity	Data fibers usage
			[Gb/s]							[Gb/s]	[%]
0	12	12	103.7	1	12	24	12	36	12	115.2	90.0
1	16	16	138.2	1	16	32	16	48	16	153.6	90.0
2	20	20	172.8	1	20	40	20	60	20	192	90.0
3	24	48	122.9	1	24	48	24	48	24	153.2	80.0
4	30	60	153.6	1	30	60	30	60	30	192	80.0
5	42	168	376.3	1	42	84	42	126	42	403.2	93.3
6	48	196	430.1	1	48	96	48	144	48	460.8	93.3
Total		520	1497.6		192	384	192	576	192	1670	

Table 2 – RUs and GBTs count, distribution and usage. Note that for layer 3 & 4 only two data fibers per RU are necessary to guarantee maximum rate operations. All capacities are referred to available payload.

1.2.3 Power Units (PUs)

Each Middle and Outer Layers stave will be powered by two identical (one for each half-stave) so-called Power Units (PU), which will translate the 12V power cable supply to the 1.8V sensor voltage by an array of CERN DC-DC rad-hard power converters (Picture Figure 11). The pair of PUs serving a stave will be controlled and managed by the RU serving the same stave

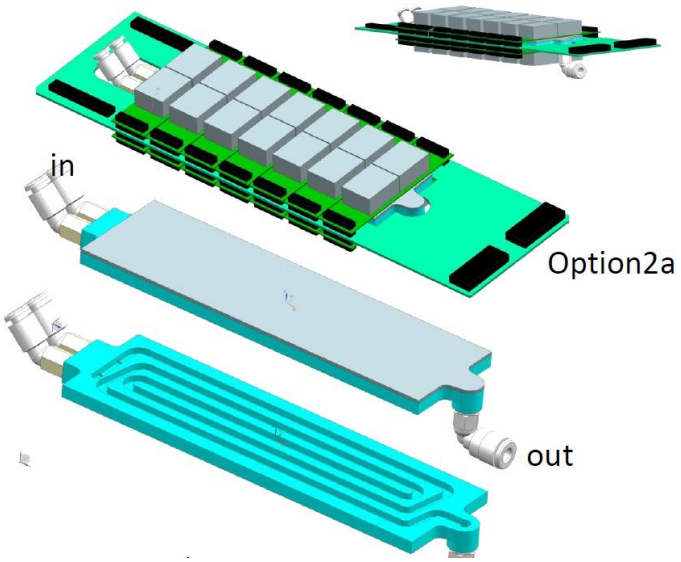

Figure 11 – Possible appearance of an Outer Layer stave power unit.

1.2.4 Busy Units (BU)

The busy status is issued by each chip in the case it is not able to complete the tasked data transmission due to internal buffer overflow or other causes, In such a case, the data flow coming from that specific chip could be completely or partially lost. As there are more than 25000 chips in the ITS, to guarantee continuous operations the system must cope with the fact that some of them will assert a busy status at every trigger/readout cycle.

The busy status from every chip has therefore to be locally collected and parsed, because transmitting it to the Central Trigger Processor would requires a too long time compared to the trigger latency (about 1.2 µs). Having a real-time picture of the whole ITS busy status is mandatory in order to asses when the number of busy chips starts affecting the physics data quality and/or to spot non-stochastic behaviours of the detector due to actual physical effects (halos in the inner layers, etc.) which may affect the chips operations.

1.3 Radiation environment

1.3.1 Overview

The readout electronic will stay in the cavern, hosted in the so-called mini frame [##]. Due to the positioning, rad-tolerant components must be considered for its implementation. The hadron fluence, quoted in 1 MeV neutron equivalents (n_{eq}), and the Total Ionising Dose (TID) are the numbers that determine the long-term radiation damage of sensors and electronics. Figure 12 and Figure 13 qualitatively illustrate the magnitude of the two effects are within the experimental volume along the beam axis for a delivered Pb-Pb luminosity of 10 nb^{-1}. The rate of hadrons with a kinetic energy > 20 MeV determines the rate of single event upsets in the microelectronics circuitry (a figure derived from the LET threshold necessary to induce an upset), and is reported in Figure 14 for 50 kHz pp-Pb collision rate.

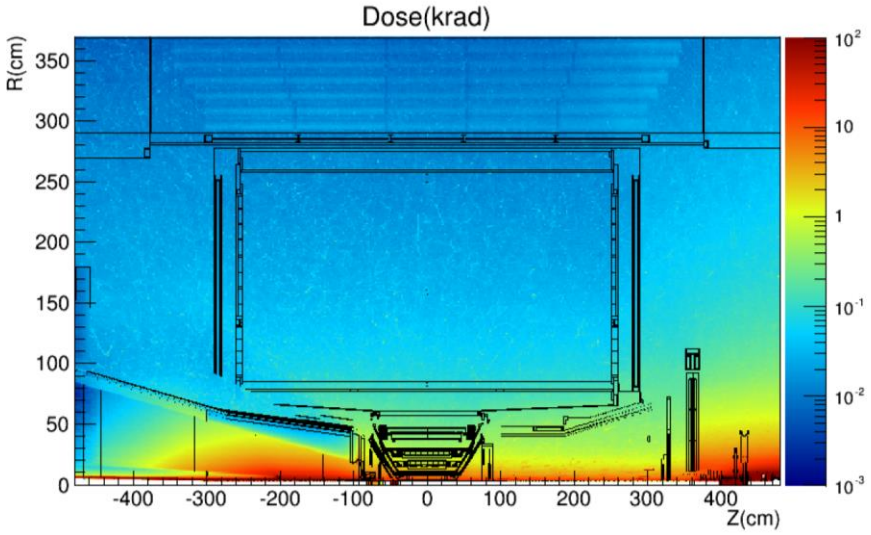

Figure 12 – Total Ionising Dose (TID) for an integrated Pb-Pb luminosity of 10 nb^{-1} in the ALICE central barrel.

At a distance of 5 meters, slightly on-axis from the collision centre, a radiation tolerance of 10 kRad and 10^{10} 1 MeV neq is still required.

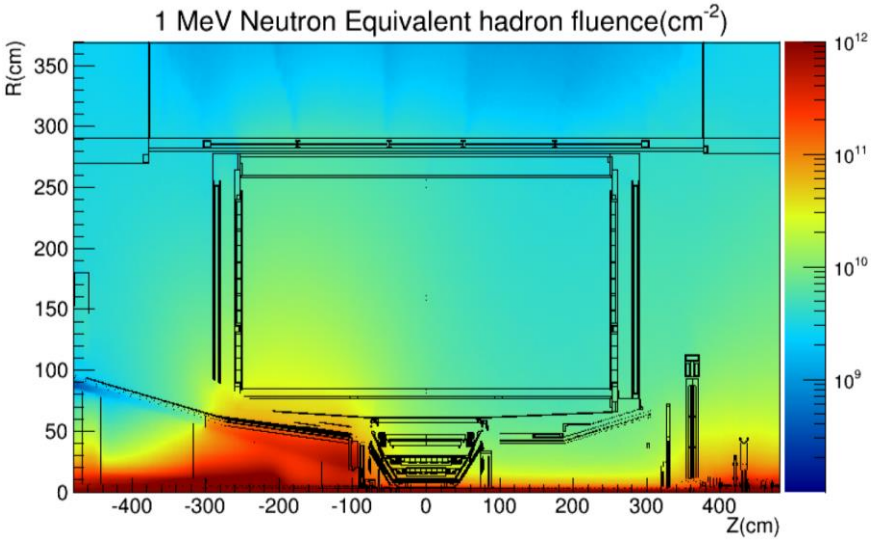

Figure 13 – Hadron fluence for integrated Pb-Pb luminosity of 10 nb^{-1} in the ALICE central barrel.

Other than adequate resistance to radiation of all passive components (cables, glues, pcbs, etc.) it is necessary that all the active components have been tested/certified for the expected radiation levels. In particular, three components must both radiation tolerant and SEU hardened:

- The power supplies, both linear and/or DC/DC. In particular, latch-up immunity is fundamental. For the foreseen TID levels, ionizing damage is not likely to be a major issue.
- The FPGAs (or equivalent COTS devices) which implement the logic functions / state machines. As for the power supplies, the biggest concern is for Single Event Effects (SEE), as TID will not likely represent an issue (but it will be anyway tested).
- The ancillary electronics (e.g. the current shunt) which complete the readout electronic.

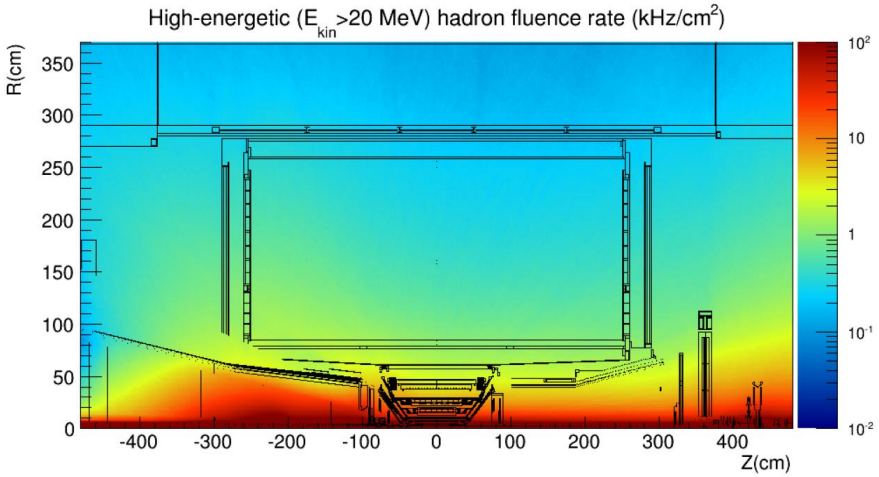

Figure 14 – High-energy (> 20 MeV) hadrons (SEE source) flux.

1.3.2 Expected radiation levels (updated at 20 Dec 2015)

Dedicated simulations [A. Alici] estimates the expected radiation levels considering both the particles generated by the primary collisions and the particles generated by beam interaction with the non-perfect vacuum within the beam pipe. Table 3 and Table 4 reports the relevant radiation levels, due to the primary interaction and the beam vacuum interaction expected for a total integrated luminosity of 13 nb^{-1} Pb-Pb interactions + 50 nb^{-1} Pb-p interactions + 6 pb^{-1} p-p interactions. Values reported in Table 3 and Table 4 have no safety-factors included.

Position respect to beam			**Radiation levels (primary collisions)**			
r	z	Reference name	TID	1 MeV n_{eq} fluence	High energy hadron flux*	Charged particle flux
[cm]	[cm]		[krad]	[cm^{-2}]	[kHz cm^{-2}]	[kHz cm^{-2}]
2.2	[-13.5 ÷ 13.5]	ITS L0	68.7 (80.3)	9.8 (10.3) × 10^{11}	765 (770)	890 (910)
43	[-73.7 ÷ 73.7]	ITS L6	0.39 (0.81)	2.2 (5.2) × 10^{10}	3.4 (4.9)	4.5 (6.7)
79	[-260 ÷ 260]	TPC In	0.14 (0.24)	2.0 (4.5) × 10^{10}	1.35 (1.8)	1.7 (3.45)
100	**330**	**RE**	**0.13**	**8.3 × 10^{9}**	**0.86**	**1.7**
258	[-260 ÷ 260]	TPC Out	0.032 (0.038)	6.2 (8.4) × 10^{9}	0.27 (0.37)	0.2 (0.3)
290	[-290 ÷ 290]	TRD	0.019 (0.025)	5.2 (7.1) × 10^{9}	0.23 (0.31)	0.15 (0.23)

- TID and 1 MeV n_{eq} fluence calculated for nominal physics program (13 nb^{-1} **Pb-Pb +** 50 nb^{-1} **Pb-p +** 6 pb^{-1} **p-p**).
- **Hadrons** and charged particle flux calculated for **50 kHz Pb-Pb** collisions (worst-case scenario).
- The average value within the z span is reported first, in brackets the peak value within the z interval.
- * Momentum > 20 MeV.

Table 3 – Expected radiation levels from primary collisions (no beam halo background)

Table 4 reports the expected radiation level assuming the vacuum quality before LS1. Vacuum improvement close to ALICE are expected to reduce those rates by a factor 10 (which is considered while computing Table 6).

Position respect to beam			Radiation levels (beam-gas collisions)			
r	Z	Reference name	TID	1 MeV neq fluence	High energy hadron flux*	Charged particle flux
[cm]	[cm]		[krad]	[cm^{-2}]	[kHz cm^{-2}]	[kHz cm^{-2}]
2.2	[-13.5 ÷ 13.5]	ITS L0	1690 (1780)	3.2 (3.3) × 1012	28.6 (30.2)	1160 (1210)
43	[-73.7 ÷ 73.7]	ITS L6	10.8 (16.5)	1.3 (3.4) × 1011	0.79 (1.2)	7.2 (9.1)
79	[-260 ÷ 260]	TPC In	2.5 (3.1)	1.2 (2.7) × 1011	0.42 (0.53)	1.7 (1.8)
100	**330**	**RE**	**≈ 2.3**	**≈ 5 × 1010**	**≈ 0.3**	**≈ 1.4**
258	[-260 ÷ 260]	TPC Out	0.36 (0.45)	3.5 (4.7) × 1010	0.09 (0.12)	0.14 (0.17)
290	[-290 ÷ 290]	TRD	0.27 (0.43)	2.9 (4.0) × 1010	0.07 (0.10)	0.09 (0.13)

- TID and fluence from beam-gas collisions assuming the vacuum conditions of Fill 2736 (average pressure 2.3 × 10-8 mbar).
- High-energy hadrons and charged particles flux are those expected for HL-LHC.
- The average value within the z span is reported first, in brackets the peak value within the z interval.
- * Momentum > 20 MeV.

Table 4 – Expected radiation levels from beam-vacuum interaction

Table 5 provides the reference values for the operating condition of the ALICE upgrade, derived by combining Table 3 and Table 4 values in the following way:

- TID values from Table 3 have been multiplied by a factor 1.3 to account for data taking inefficiency.
- TID values from Table 4 have been divided by a factor 10 to account the vacuum improvement after LS1.
- Resulting TID values have been summed and the multiplied by a safety factor 10.
- For the charged hadrons rate, the Pb-Pb only values have been used, as the Pb-Pb and p-p operation are mutually exclusive, with the primary Pb-Pb contribution being the major one, while the higher beam-halo interaction rate of p-p operation is paired to a negligible primary.
-

Position respect to beam			Radiation levels (total)			
r	z	Reference name	TID	1 MeV n_{eq} fluence	High energy hadron flux*	Charged particle flux
[cm]	[cm]		[krad]	[cm^{-2}]	[kHz cm^{-2}]	[kHz cm^{-2}]
2.2	[-13.5 ÷ 13.5]	ITS L0	2734	1.7 × 1013	765 (770)	890 (910)
43	[-73.7 ÷ 73.7]	ITS L6	20	8.1 × 1011	3.4 (4.9)	4.5 (6.7)
79	[-260 ÷ 260]	TPC In	5.6	7.0 × 1011	1.35 (1.8)	1.7 (3.45)
100	**330**	**RE**	**≈ 5**	**≈ 1.6 × 1011**	**0.86**	**1.7**
258	[-260 ÷ 260]	TPC Out	0.86	1.4 × 1011	0.27 (0.37)	0.2 (0.3)
290	[-290 ÷ 290]	TRD	0.6	1.2 × 1011	0.23 (0.31)	0.15 (0.23)

- TID & fluence = (Table 3 × 1.3data taking efficiency + Table 4 / 10 better vacuum) × 10 safety factor.
- Safety factor of 10 on top of TID and fluence calculated as in the above line.
- Hadrons and charged particles as for 50 kHz Pb-Pb collisions (Table 3, worst-case scenario).
- The average value within the z span is reported first, in brackets the peak value within the z interval.
- * Momentum > 20 MeV.

Table 5 – Expected TOTAL radiation levels

2 System operations

2.1 Sensor operations

2.1.1 Pixel cell overview

Being the first and most critical element of the whole transduction chain, the sensor behaviour obviously drive the strategy to optimize the readout chain. A key point to understand how the sensor works is to recall that the analogue circuitry (front end and shaper) in the pixel cell is always active and trigger-less. This design solution has been adopted in order to minimize power consumption by avoiding to distribute any high frequency clock through the matrix. To further minimize power consumption, the analogue stage is relatively "slow", whit a shaping time (called pulse length) of about 2 µs. Yet this figure is only indicative, it sets the scale of issue. Therefore, when a particle release charge in the pixel cell, a signal rise and fall at the shaper output, whichever operating status the sensor is (Figure 15). A comparator translate the shaper output into the digital domain, asserting a '1' the whole time the analogue signal stays over a programmable threshold.

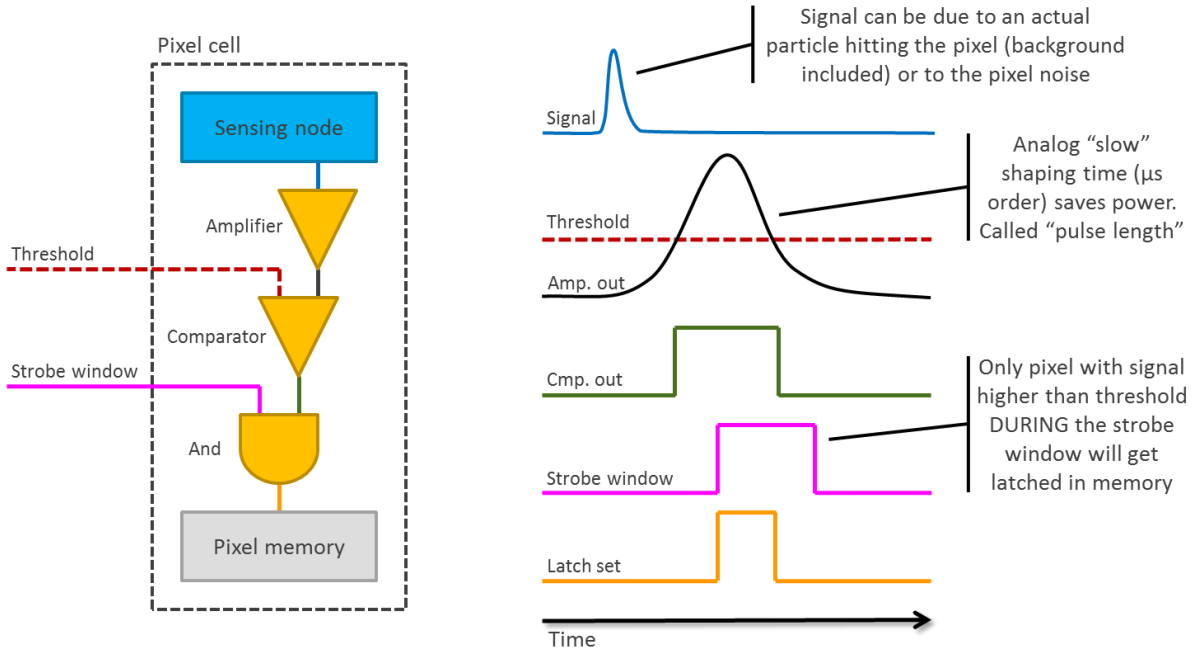

Figure 15 – Pixel logic schematic and timing diagram.

An external digital pulse simultaneous for all pixels in the matrix, called strobe, latches the comparator output of each pixel into the pixel cell buffer. In this way an 'image' of the matrix can be stored in memory, and later retrieved and sent outside the sensor. To improve the data throughput the sensor can handle, every pixel will actually embed more than a single bit buffer, most likely three.

2.1.2 Data latching

The 'long' analogue shaping time and the 'strobe' signal behaviour have important implications in the practical way the sensors operates. The strobe main purpose is to operate the sensor in triggered mode, i.e. saving in memory the entire matrix image every time the strobe is asserted as consequence of a trigger arriving from the outside. The trigger will arrive with a defined trigger latency respect to the actual physics event (the particle passing through the detector), but as long as this latency is shorter than the analogue shaping time, the signal generate by the physic events will be still high when the trigger-activated strobe arrives, and therefore the hit will be recorded into the pixel buffer. This situation is exemplified in Figure 16, where two physics events (collisions with relevant data, red lines on lower graph) generate two triggers delayed in time by the trigger latency (pink lines on lower plot). The triggers in turn drive the strobe signal, during which window (strobe window in figure) every signal over the threshold is stored into the buffer. In

the example, the first trigger (#0) records the first physical event into the matrix memory, but the second trigger (#1) actually records both physics events (#0 and #1) into a new buffer.

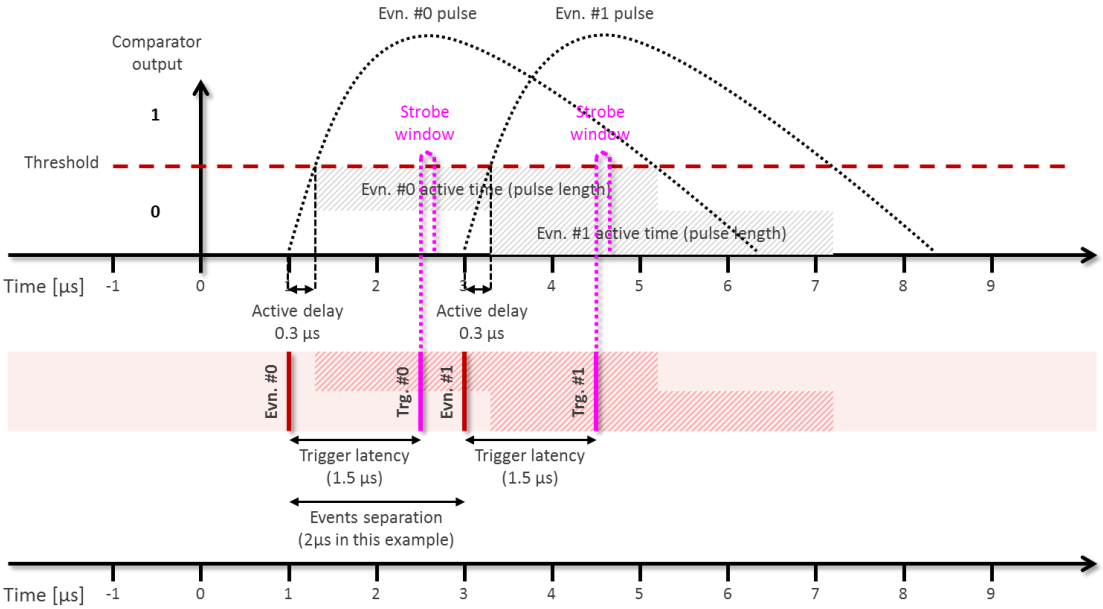

Figure 16 – Event #0 is double latched due to analogue shaping time (pulse length).

The result is that physics event #1 has been recorded twice, which is a direct consequence of the analogue shaping time. For triggers farther apart than the typical shaping time (≈2µs), the sensor operates as expected and stores only one physical event per strobe window.

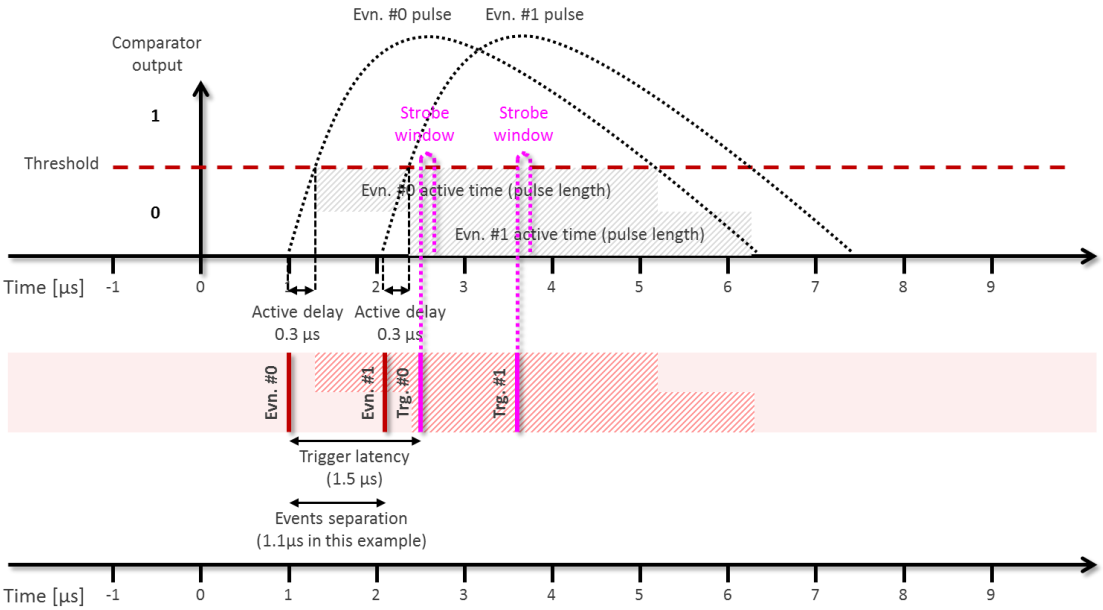

Figure 17 – Event #1 is already latched by trigger #0 due it happens less than a trigger latency after event #0.

The example already illustrates one condition which leads to record more data than what necessary, and quantitative measure of this will be shown in the simulation section (**Error! Reference source not found.**). In act the shaping time provides a sort of analogue memory which retains the information of an event for the time necessary for the trigger to confirm the event relevance, this time being the trigger latency. Such timing lead also to the situation illustrated in Figure 17, which exemplify why it is un-necessary to send to the sensor triggers closer in time than the trigger delay itself. If two physics event are separated in time by less than the trigger latency (minus the rise time necessary for the signal to pass the comparator threshold, called active delay). Whichever event happens during the trigger latency period (minus the active delay time) is in fact

stored in memory at the arrival of the trigger, therefore rendering useless processing its own trigger, which will only duplicate it in memory.

2.1.3 Matrix Readout

Once the strobe signal stored the matrix signals into the current buffer, a readout procedure start to read out all the data from the matrix. The priority encoder readout circuit crawls in each column to extract the address of those pixel with a latched '1', and it does it in $\log_2 n$ steps, where n is the pixel count in a column. This ensure an extremely fast readout time of the matrix, which varies depending of the priority encoder implementation (see **Error! Reference source not found.**), but it is anyway equal or less of than 100 ns. Data re stored into a main buffer memory, where they wait to be sent through the high-speed differential line.

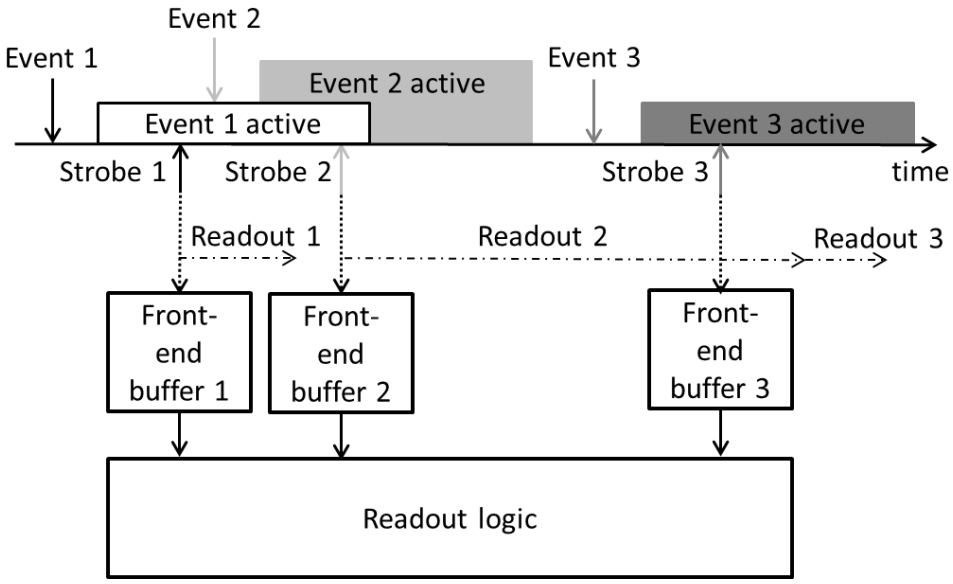

Figure 18 – Sensor readout scheme.

2.1.4 Data bandwidth

The amount of data a sensor collects depend of its position inside the ITS, on the average interaction rate, on the interaction type and on the noise the sensor itself generates. Sensors closer to the interaction point will intercept more particles, thereby generating more data, which amount obviously shows an almost square radius dependence. Higher the interaction rate, higher the data throughput generated by the sensor per unit of time and area. Innermost sensor will also record background particles trapped into the magnetic field, as well as beam halos and other potential background sources, while outer sensors will not be affected by such background events. Like physics events background events increases with the average interaction rate. The sensor itself generates its own amount of noise data, i.e. pixel which randomly fire as they were hit by a particle in absence of any actual signal. The noise is independent on the sensor position in the ITS. The interaction type (Pb-Pb or p-p) strongly influence the data throughput, as each Pb-Pb event generates much more tracks than a p-p event, leading to higher data bandwidth for the same interaction rate.

As pixel comparator status is latched into the buffer during the strobe window period (Figure 15), the longer the strobe stay open the more likely background events will be latched as well, increasing the recorded unwanted signal. As far it concern the noise, its dependence on the strobe window width depend on the specific sensor, and must be experimentally evaluated. Figure 19 gives a graphical representation of the situation. On the lift, three main bands show the physics events (collisions, in red), the background events (trapped particles, halos, etc, in yellow) and the sensor generated noise (in blue) happening in time, while the pink bar represents the trigger signal. The strobe windows encompasses events prior to the trigger signal itself due to the analogue memory effect, as discussed in the previous section. On the right, the contribution of each signal source to the total data throughput is represented (loosely to scale). The dark grey box represents the protocol necessary to encode the information, while the striped box is the overhead due to the encoding scheme (8/10, hence 20% of the total payload).

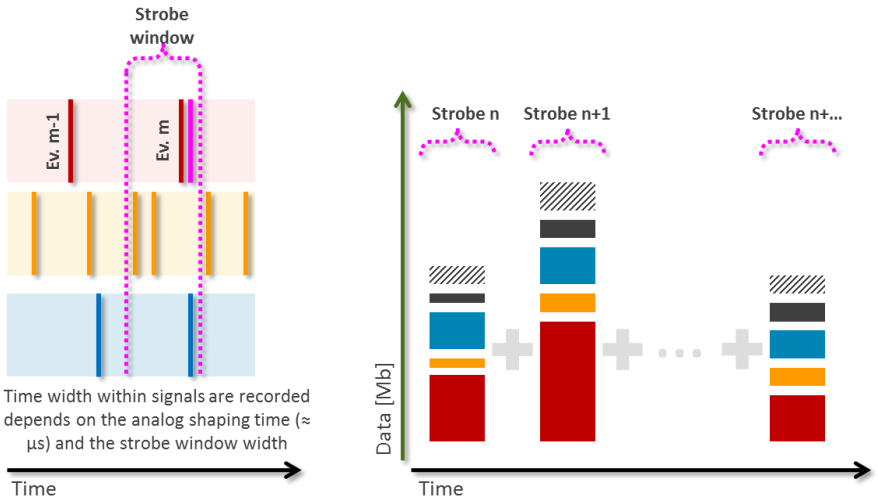

Figure 19 – Signals recorded by the sensor during the strobe window and their contribution to the data throughput.

Representation of Figure 19 is just a pictorial one intended to illustrate the idea, while real figures are reported in section **Error! Reference source not found.**. Using the same color coding, Figure 20 approximate the different data throughput composition expected for the different layers and different interaction types. It is easy to see the different impact to the data throughput of a Pb-Pb event respect to a p-p event, especially in the Inner Layers. In the Outer Layers instead, the noise is playing the major role in defining the system data throughput, regardless the interaction type.

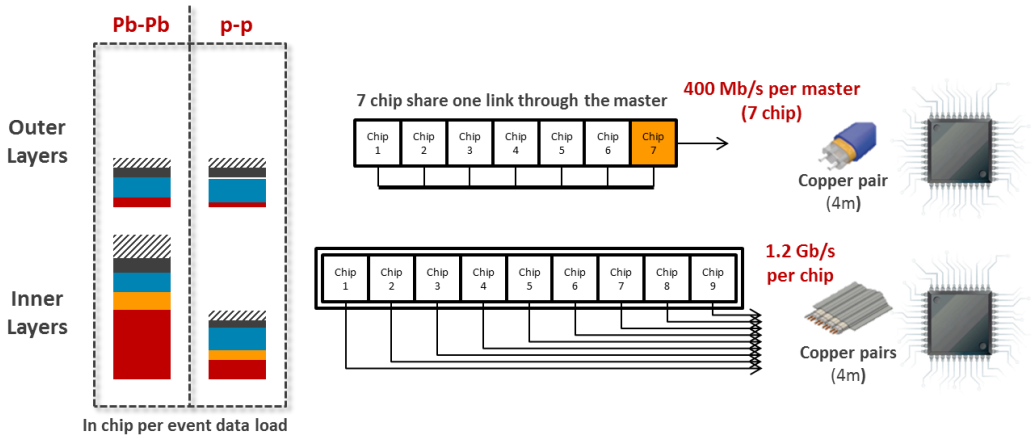

Figure 20 – Data throughput composition for different layers and interaction types.

2.2 Sensor protocols

2.2.1 Trigger

2.2.2 Control

2.2.3 Data

The data output is unidirectional from the sensor, through the high-speed serial line, which support 1.2 Gb/s data rate for the Inner Layers and 400 Mb/s data rate for the Middle and Outer Layers. Additionally, in the Middle and Outer layer only the master chip is connected to the high speed line, and a token-ring shared local bus is used to alternatively connect one chip to the high speed driver [pALPIDE3 ref]. Table 6 lists all the code used by the pALPIDE3 chip in the output data stream.

Code	Length	Binary code
NOP*	8 bits	1111_1111
IDLE	8 bits	1111_0000
BUSY_OFF	8 bits	1111_0010
BUSY_ON	8 bits	1111_0001
REGION_TRAILER*	8 bits	1111_0011
CHIP_EMPTY_FRAME	16 bits	1110_<chip_id[3:0]><frame_id[7:0]>
CHIP_FRAME_HEADER	8 bits	1010_<chip_id[3:0]>
CHIP_FRAME_TRAILER	16 bits	1011_<chip_id[3:0]><frame_id[7:0]>
REGION_HEADER	8 bits	110_<region_id[7:0]>
DATA_SHORT	16 bits	00_<hit_position[13:0]>
DATA_LONG	24 bits	00_<cluster_position [13:0]><cluster_map[7:0]>

* These codes are used in the module local bus only

Table 6 – Data output codes for the pALPIDE3 chip.

In response to a trigger (either external or internal in case of continuous mode) the chip retrieves the data from the matrix memory [pALPIDE ref] and send them in a *data frame*:

- CHIP_EMPTY_FRAME is the chip data frame in case of no hits.
- A non-empty frame begins with CHIP_FRAME_HEADER, contains at least 1 and up to 32 Region Data Frames. It ends with a CHIP_FRAME_TRAILER.

A *Region Data Frame* (32 per chip) is organized as follows:

- Block of hit data read-out from 32 sections of the ALPIDE Matrix REGION_HEADER codes transmitted as prefix of Region Data Frame.
- Regions with no hits do not generate Region Data Frames.
- Region Data Frame contain variable length, mixed sequences of DATA_SHORT or DATA_LONG code words. DATA_SHORT are used for 'single pixel hits', DATA_LONG are used for clusters of neighbor hits.

An *Event Data Frame* is a block of data transmitted on one high speed link in correspondence of one trigger or at the end of an integration window. Its composition varies for the Inner Layers and the (Middle and Outer Layers:

- The Inner Layers (single chip) *Event Data Frames* are made of one Chip Data Frame.
- The Outer Layers (master chip plus slaves) *Event Data Frames* are sequences of (up to) 7 Event Data Frames.

Chip Data Frames of Slave chips are received by the Master on the local bus and forwarded sequentially to the Readout Electronics

IDLE codes are allowed but not required between other valid codes

Optional BUSY_ON/BUSY_OFF codes are allowed between other valid codes

Codes that are 2 bytes or 3 bytes CAN NOT be split by IDLE or BUSY_ON/BUSY_OFF

2.3 Triggered operation

2.3.1 Timing

In the triggered mode, the strobe signal which stores the matrix status is driven by an external trigger, issued whenever a physic event has been deemed worth to save. The average event rate indicates the average number of interactions per second, and assumes a Poissonian trigger distribution over time. Figure 21 schematizes the triggered operation mode. Vertical bars represent pixel firing due to a particle from an interaction (physics event, red), pixel firing due to a background particle (background event, yellow), or pixel firing without being hit (blue, sensor noise). The shadow area after the bar illustrates graphically the period the signal in the pixel remains high (logical '1' at the comparator output) due to the shaping time. The pink trigger line is a trigger which forces to latch the current pixel state within the strobe window (here exaggerated in width). The trigger always follow the physical event (by the trigger latency), but data event are not lost due to the analogue delay.

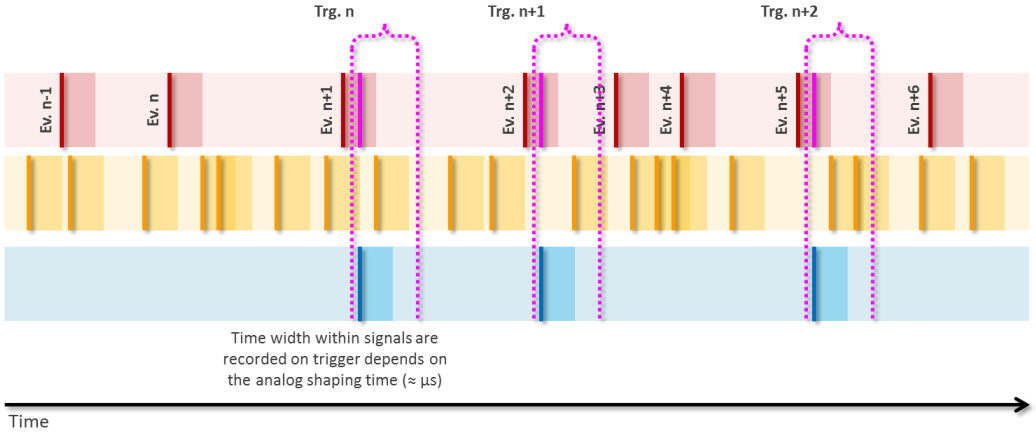

Figure 21 – Triggered operation timing.

2.3.2 Trigger management

As discussed and illustrated in Figure 17, there is no reason to pass to the detectors triggers closer in time than the trigger latency. Therefore, the Readout Electronic must handle the triggers and decide whether to send them or no to the sensor accordingly to the latest issued trigger. A trigger is passed only if enough time has passed since the previous one (this time being equal to the *trigger latency* minus *active delay* and *other delays*).

Figure 22 –Readout Electronic trigger filtering.

In case of a trigger being halted because another one has been issued within the trigger latency window, the readout electronic stores the trigger arrival, timestamp it and queue it. Also the triggers actually sent to the detector are time/stamped and queued. This way the Readout Electronic can associate all the triggers arrived during the time period actually recorded by the matrix at the time the strobe signal is asserted.

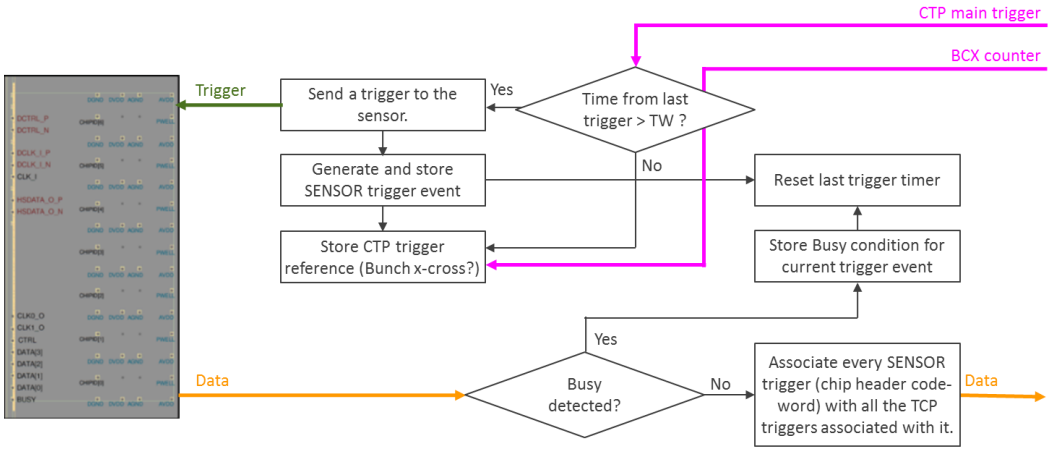

Figure 23 – Trigger filtering logic.

Figure 24 summarizes the trigger timing between the RU and the chip. Triggers which arrive closer in time than the trigger latency (the dotted horizontal purple line beneath the first time-strip) are not passed to the chip, but stored in memory. The only triggers passed to the chip (green vertical lines, second time-strip) are therefore spaced in time of at least a trigger latency. Trigger passed to the chip are marked by a simple circular trigger ID (3-4 bits) generated by the RU. Data packets coming back from the chip contains (in the trailer or in the header) the trigger ID, allowing the RU to check for any missing data and/or to verify the data flow in case of busy/error flag from the chip.

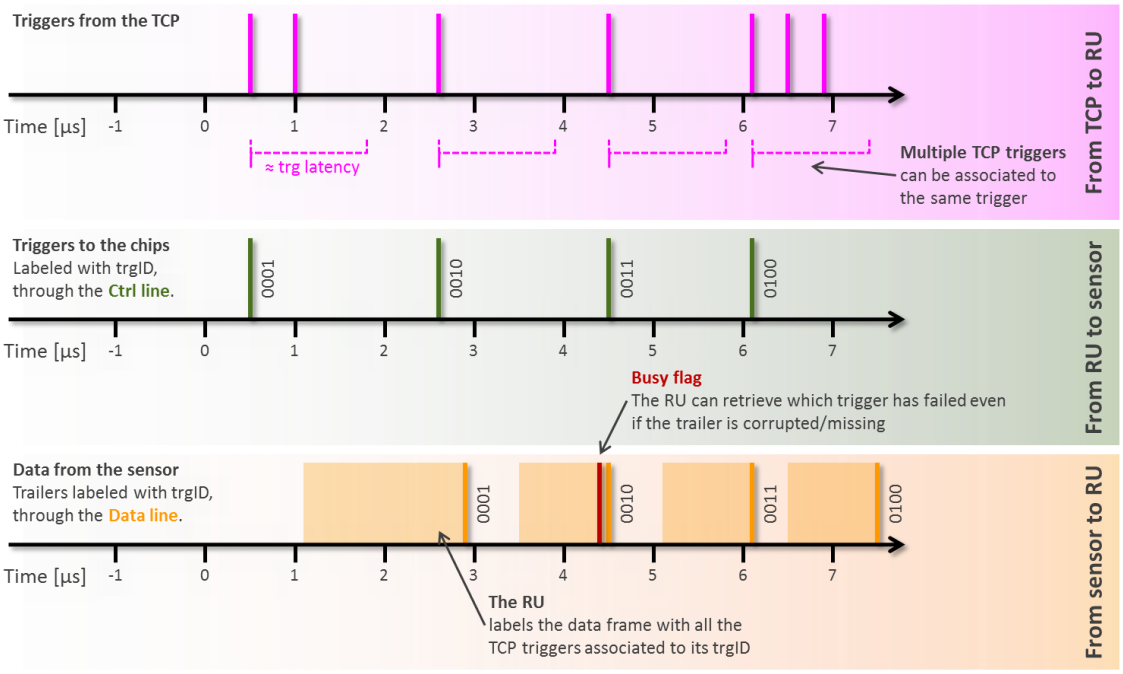

Figure 24 – Timing representation of trigger filtering. All the triggers happening inside the trigger delay are bounded to a single trigger sent to the chip. The data generated by this chip-trigger are then labelled with all the CTP triggers associated with it.

2.4 Continuous operation

2.4.1 Timing

The continuous readout mode uses the very same strobe signal of the triggered acquisition, only keeping it "on" for the length of a frame, therefore following a fixed time pattern regulated (or simply synchronized) by some external signal (heartbeat). The heartbeat signal could set the actual frame length (hence the readout frequency), or it could be used to keep in synch across the whole ITS bunch of frames generated by internal timing of the sensors themselves. As for the triggered mode, Figure 25 schematizes the continuous

operation mode. Vertical bars represent pixel firing due to a particle from an interaction (physics event, red), pixel firing due to a background particle (background event, yellow), or pixel firing without being hit (blue, sensor noise). The shadow area after the bar illustrates graphically the period the signal in the pixel remains high (logical '1' at the comparator output) due to the shaping time. The pink lines enclose frames, i.e. the strobe staying "on". During this period, whichever event happens is stored into the matrix buffers. At the end of the integration time, the strobe is de-asserted and the readout starts. As soon as the readout started, the strobe is re-asserted and the cycle starts again.

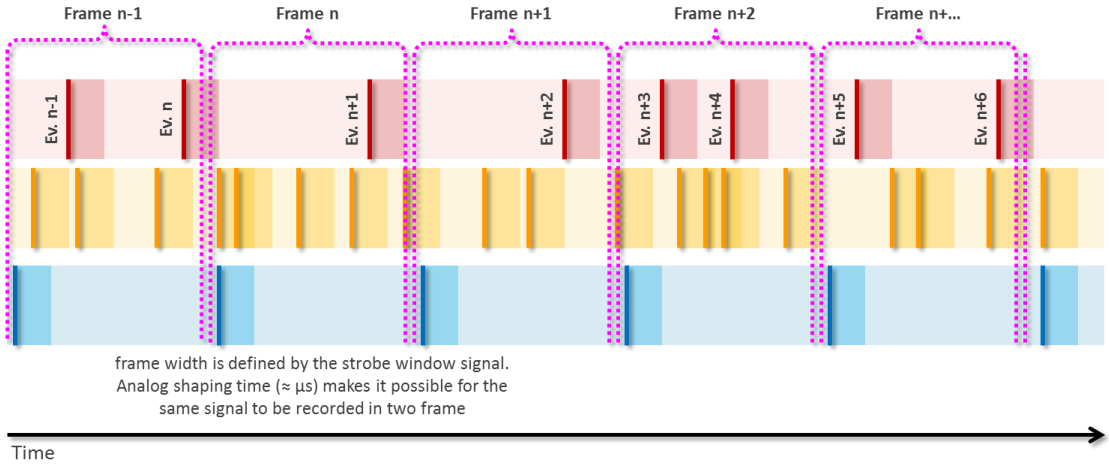

Figure 25 – Continuous readout time structure.

The strobe stays de-asserted for a minimal time (10s of nanoseconds), as the multiple in-pixel buffer allow to readout one buffer set while the current events are saved into other one.

In this configuration the frame rate is essentially limited by the available bandwidth, not by the sensor internal memory or readout architecture.

3 Performance simulations

For both the Triggered and Continuous mode discussed in section 2 and for Pb-Pb and p-p interaction extensive simulations have been carried using a system-c environment which models all the relevant part of the readout chain, including the sensor digital periphery. Common to all the following sub sections is some terminology (which is the same used through other part of this document):

- Frequency: the stated frequency always refers to the average interaction rate, whichever Pb-Pb or p-p.
- Buffers number: the number of buffers (1 bit each) present in each pixel cell.
- Internal memory: number of memory words available at the matrix periphery. The number indicates how many words are available per region (the matrix is divided into 32 regions).
- Noise: the probability of a pixel carrying a signal due to sensor noise at each readout cycle (strobe asserted and de-asserted).
- Pulse length: the average time of a signal staying over the comparator threshold, closely related (and here synonym for simplicity) to the analogue stage shaping time.
- Priority encoder period: the duration it takes to transfer the data from the pixel buffer to the periphery memory. After this time, the pixel buffer are ready to store another set of data.

3.1 "Physics events" rates

The estimated data throughput generated by the ITS is gathered by simulating the full behaviour of the detector (sensors and readout electronic) when fed with data from the physics simulations [##].Table 7 summarizes the hit densities for the different layers for minimum bias events.

		Pb-Pb			p-p	
Layer	Radius	Prim. & sec. particles **average** [a]	Prim. & sec. particles **max** [a]	QED electrons [b]	Prim. & sec. particles **average** [c]	Prim. & sec. particles **max** [c]
	[mm]	[cm^{-2}]	[cm^{-2}]	[cm^{-2}]	[cm^{-2}]	[cm^{-2}]
0	22	8.77	12.45	6.56	0.08	0.11
1	31	6.17	8.61	3.39	0.05	0.07
2	39	4.61	6.19	1.84	0.04	0.05
3	196	0.34	0.45	0.01	0.00	0.00
4	245	0.24	0.31	0.00	0.00	0.00
5	344	0.13	0.17	0.00	0.00	0.00
6	393	0.11	0.13	0.00	0.00	0.00

[a] hit densities in Pb-Pb collisions (minimum bias event, including secondaries due to material)
[b] for an integration time of 10 μs, a Pb-Pb interaction rate of 50 kHz, a magnetic field of 0.2 T (worst case scenario) and $p_T > 0.3$ MeV/c.
[c] hit densities in central p-p collisions (including secondaries produced in material)

Table 7 – "Physics events" rates for minimum bias events.

3.2 Overall maximum performance

3.2.1 Triggered mode

Table 8 illustrates the maximum average trigger rate sustainable in trigger mode, i.e. the average trigger rate at which the data lost is less than 1%. A faster trigger rate implies a (quickly) increasing data loss.

Reported results did not change for a 25 ns or 50 ns period priority encoder, while a 100 ns period would affect the reported figures. The noise level is relevant only for the Outer Layers, as the Pb-Pb events generates the majority of pixel hits.

Interaction	Noise [/px]	Inner Layers	Outer Layers
Pb-Pb	1×10^{-5}	190 kHz	195 kHz
	1×10^{-8}	190 kHz	195 kHz
p-p	1×10^{-5}	900 kHz	500 kHz
	1×10^{-8}	900 kHz	900 kHz

Table 8 – Maximum average trigger rate in triggered mode. 256 word memory, 3 buffers per pixel, 25 ns priority encoder period (40 MHz).

3.2.2 Continuous mode

Table 9 summarizes the relative data loss (1 = 100%) expected in continuous mode depending on the different frame rate, interaction type and frequency, and noise level. 1 µs frame length has been report for reference only, as it is meaningless to integrate for a much shorter time than the analogue shaping time itself. The row reporting 200 kHz Pb-Pb interaction has been also added for reference, as it is not foressen to run at such interaction frequency with heavy ions.

At 2 µs frame length (500 kHz frame rate) the priority encoder period became a critical parameter for 2 µs frame length in the Inner Layers, whichever the noise level: a 25 ns period lead to irrelevant data loss, while a 50 ns period rises the data loss about to 5%. At 5 µs and 10 µs frame length the data loss is negligible in both The Inner and Outer Layers, whichever the interaction type.

		Frame length (strobe window)							
		1 µs		2 µs		5 µs		10 µs	
Interaction type and rate	Noise [/px]	IL	OL	IL	OL	IL	OL	IL	OL
Pb-Pb @ 100 kHz	1×10^{-5}	0	0.4	0, 0.05	<0.01	0	0	0	0
	1×10^{-8}	< 0.2	<0.01	0, 0.05	0	0	0	0	0
Pb-Pb @ 200 kHz	1×10^{-5}	0.5	0.35	0.3	0.1	0.11	<0.01	0	0
	1×10^{-8}	0.5	0	0.3	<0.01	0.11	0	0	0
p-p @ 1 MHz	1×10^{-5}	0	0.2	0	<0.01	0	0	0	0
	1×10^{-8}	0	0	0	0	0	0	0	0

Table 9 – Continuous mode, data loss rate depending on interaction type, interaction rate, noise level and frame length. 256 word region memory, 3 buffers per pixel, 25 ns priority encoder period.

3.2.3 Maximum operating rates

Data rates for Pb-Pb and p-p interaction have been simulated for various interaction rates and sensor noise levels. While simulations have been carried out considering a wide range of possible sensor configurations (periphery memory size, internal encoding speed, etc.) and operational parameters, the results reported in this note refer to the most likely final sensor implementation and usage. Table 10

illustrates the maximum average interaction rates the ITS is foreseen to sustain when operating in triggered or continuous mode.

Interaction type	Triggered	Continuous		
		5 μs frame	10 μs frame	20 μs frame
Pb-Pb	up to 150 kHz	up to 150 kHz	up to 200 kHz	up to 200 kHz
p-p	up to 200 kHz	up to 1 MHz	up to 1 MHz	up to 1 MHz

Table 10 – Maximum sustainable interaction rates.

The actual data throughput produced for a given operational condition will vary depending on the noise level of the sensors. In the next two section simulations of the expected total data rates for Pb-Pb and p-p-interactions are detailed. Data rates breakdown fitting the actual readout topology and a quick overview of the readout system itself are provided in section 3.6.

3.3 Sensor parameter simulation

During the sensor design phase, a wide parameters space has been explored in order to determine the optimal sensor configuration respect the design interaction rate and expected noise level. A few example are here reported for the triggered mode only in order to exemplify the influence of the different design parameter on the overall system performance.

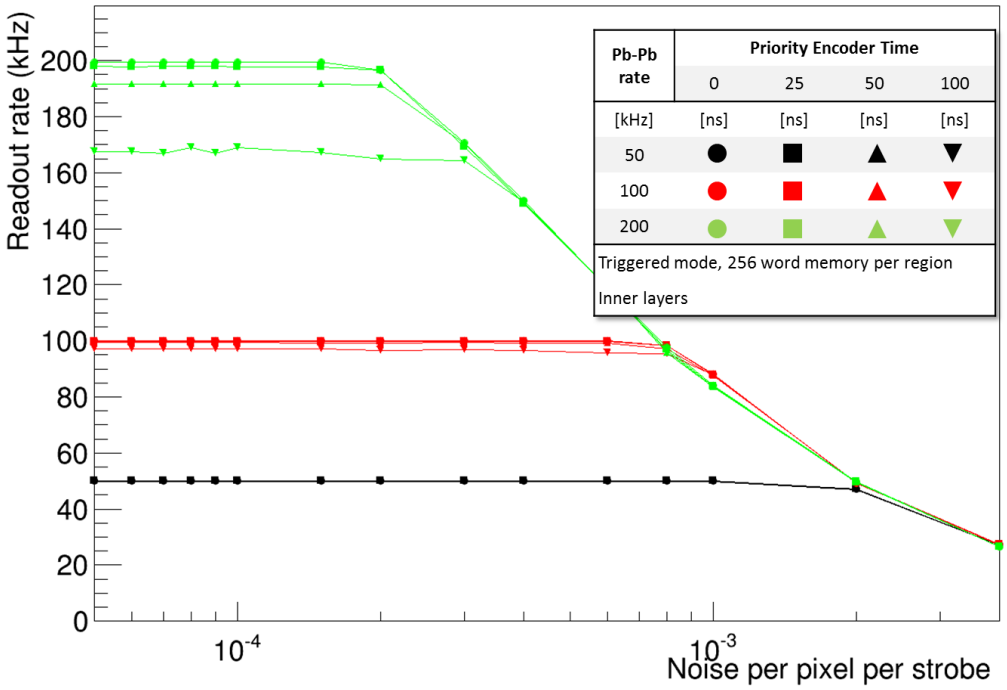

Figure 26 – Pb-Pb collisions in the **1st layer** from 50 kHz to 200 kHz average rate in triggered mode. The readout rate should match the average trigger rate, but it fails whenever the noise rate is too high and/or the time required to read out the matrix (Priority Encoder time) is too long.

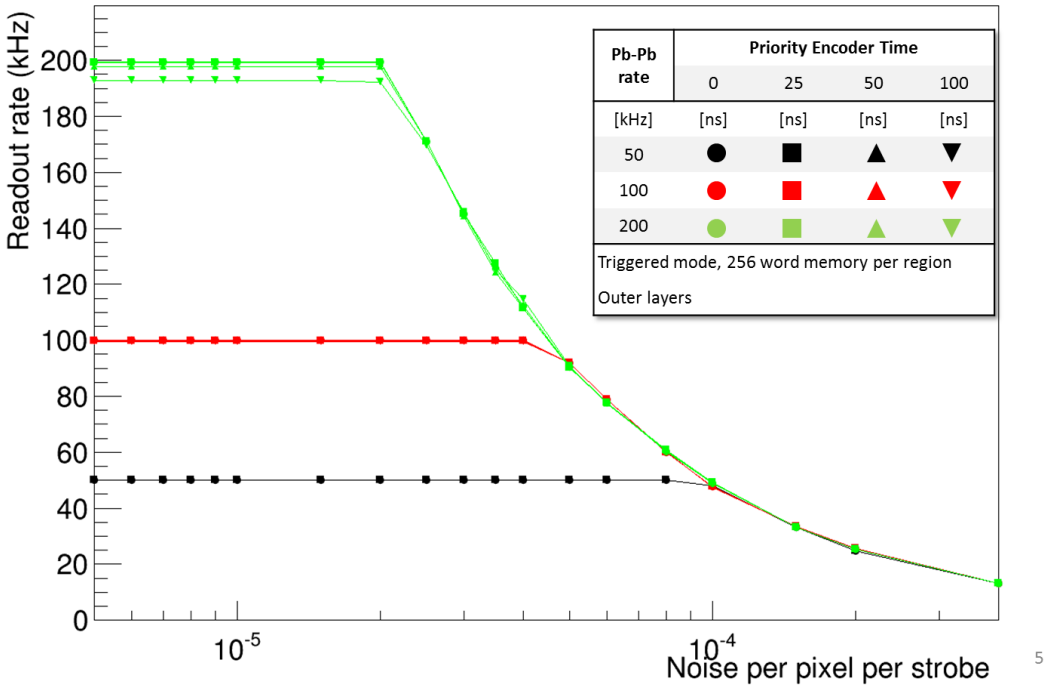

5

Figure 27 – Pb-Pb collisions in the **4th layer** from 50 kHz to 200 kHz average rate in triggered mode. The readout rate should match the average trigger rate, but it fails whenever the noise rate is too high and/or the time required to read out the matrix (Priority Encoder time) is too long.

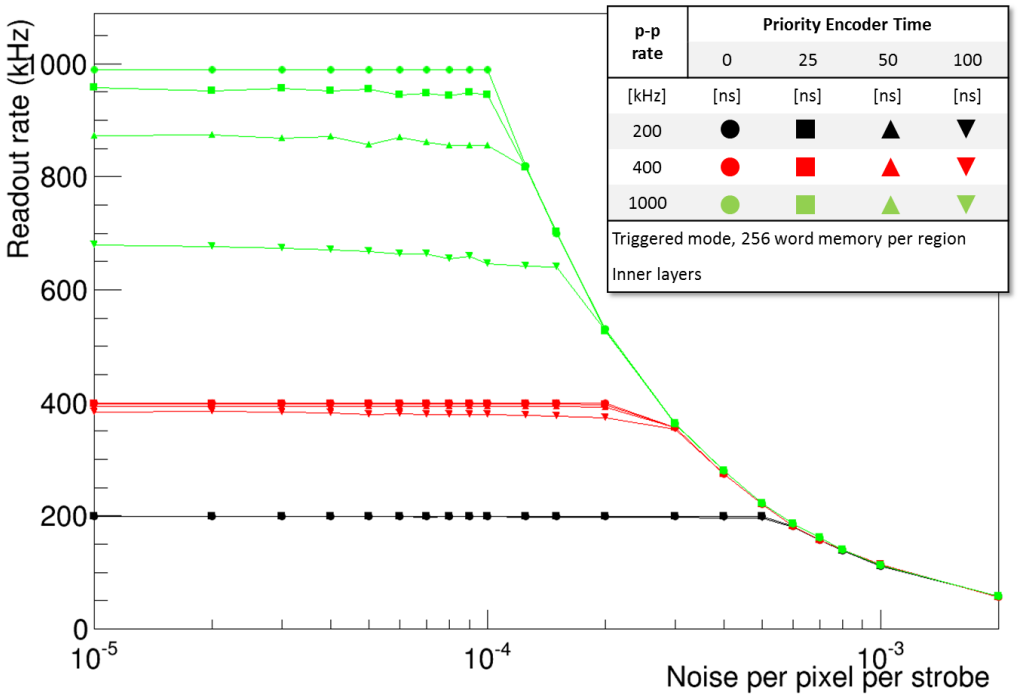

Figure 28 – p-p collisions in the **1st layer** from 200 kHz to 1000 kHz average rate in triggered mode. The readout rate should match the average trigger rate, but it fails whenever the noise rate is too high and/or the time required to read out the matrix (Priority Encoder time) is too long.

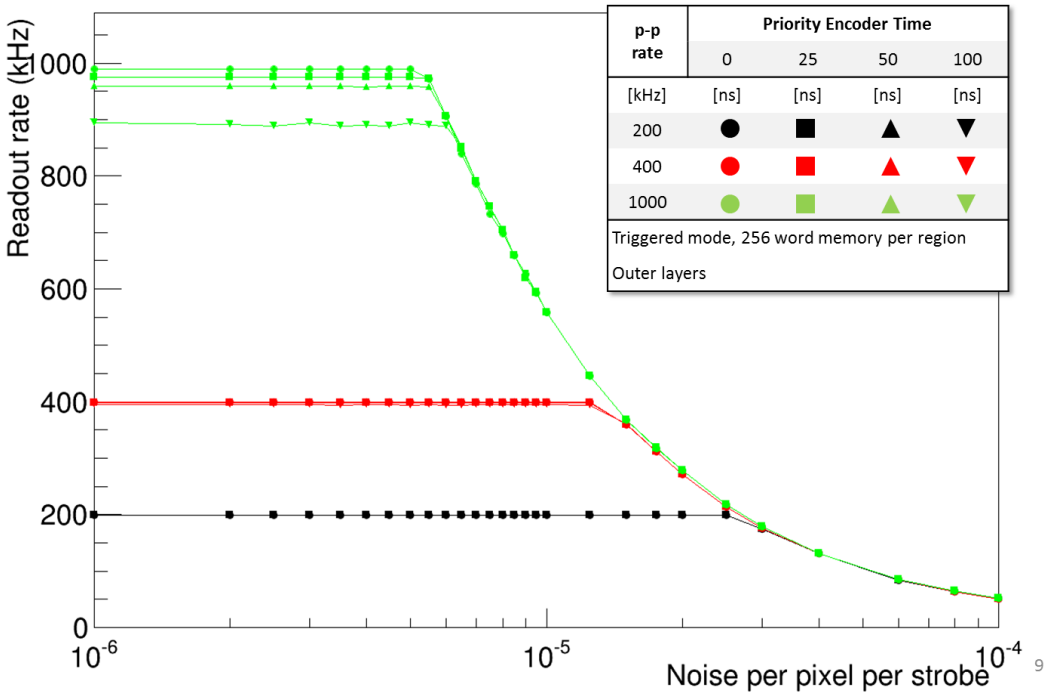

Figure 29 – p-p collisions in the **4th layer** from 200 kHz to 1000 kHz average rate in triggered mode. The readout rate should match the average trigger rate, but it fails whenever the noise rate is too high and/or the time required to read out the matrix (Priority Encoder time) is too long.

3.4 Pb-Pb total data rates

Rates are expressed in Gbit/s for the full ITS. The orange part of the bar represents the actual hit addresses, while the pattern stripes atop shows the protocol overhead from the detector to the Readout Electronic. The total required bandwidth is the sum of the two. It is foreseen to reduce the protocol overhead in the Readout Electronic before sending the data to the CRU/O2. Data are reported for a 5 µs and 10 µs shaping time, the increase of data rate respect to a 2 µs shaping time not being relevant (unless for 200 kHz Pb-Pb collisions, see Figure 33). Values have been reported for two noise levels, 10^{-5} and 10^{-6} px^{-1}, which represents the worst case scenario and the optimal scenario respectively. Better noise figures (< 10^{-6}) further reduce the data rate marginally, and are omitted from the graphs for clarity.

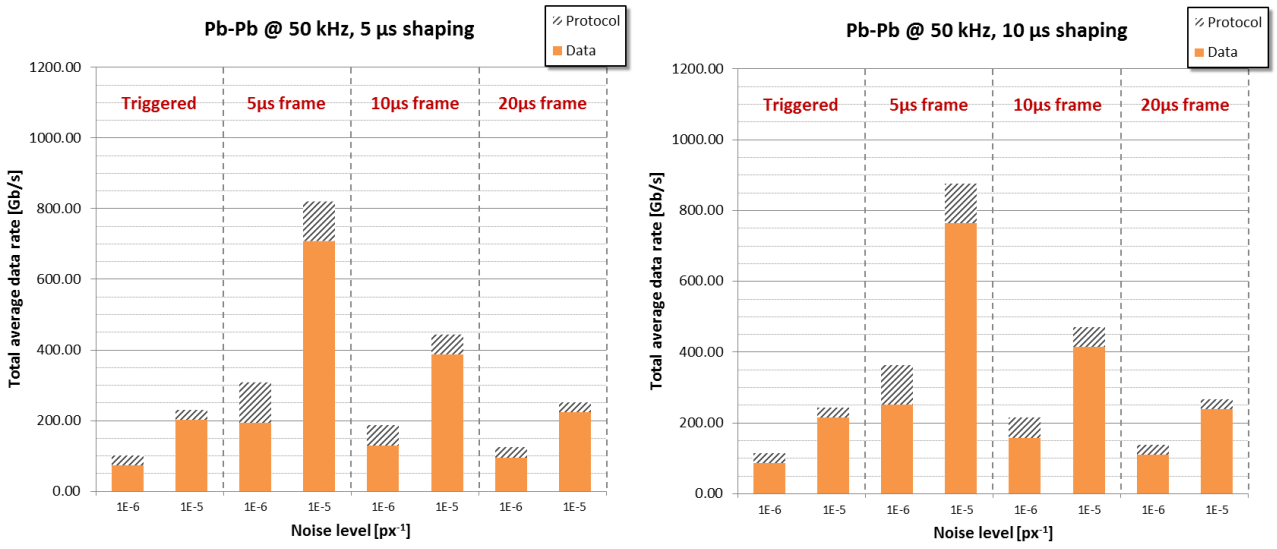

Figure 30 – Pb-Pb @ 50 kHz, 5 µs and 10 µs shaping.

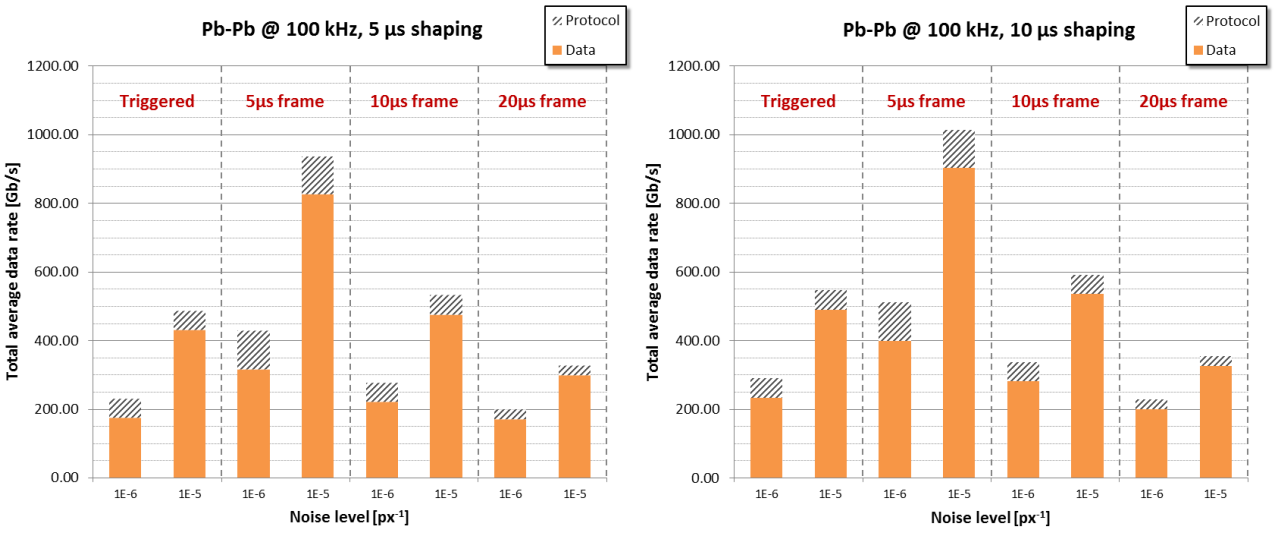

Figure 31 – Pb-Pb @ 100 kHz, 5 µs and 10 µs shaping.

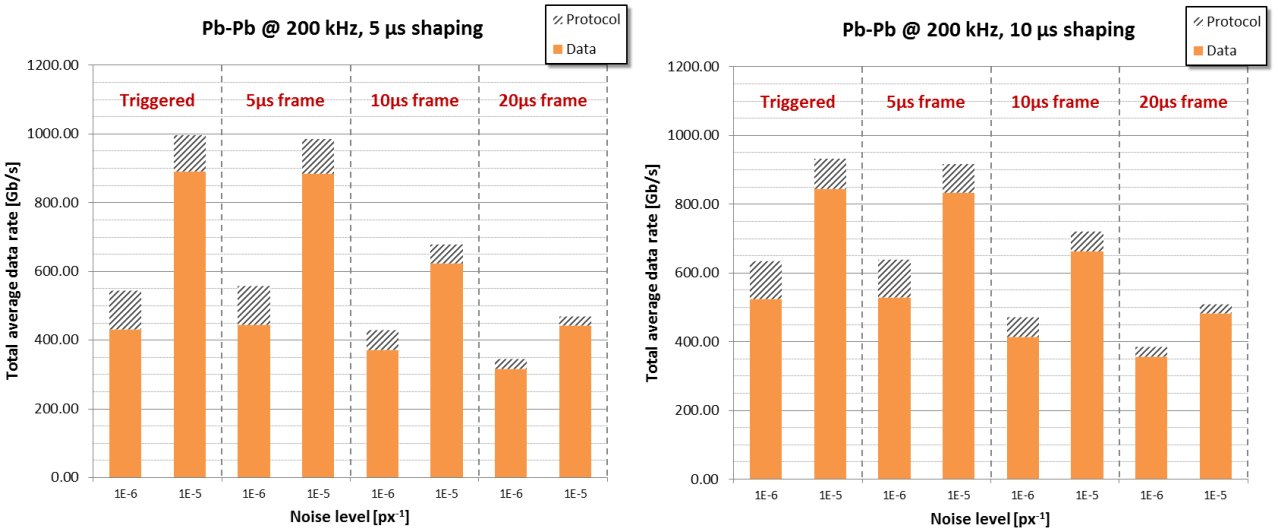

Figure 32 – Pb-Pb @ 200 kHz, 5 µs and 10 µs shaping.

For Pb-Pb collisions @ 200 kHz the data rate is reported also for a 2 µs shaping time (Figure 33), as the effect on the data rate is important at those interaction frequencies (about 30% less data throughput respect to a 10 µs shaping time in the low-noise condition). It has to be remarked that at the time of this note last revision the 2 µs shaping time is not considered a baseline operating condition of the sensor.

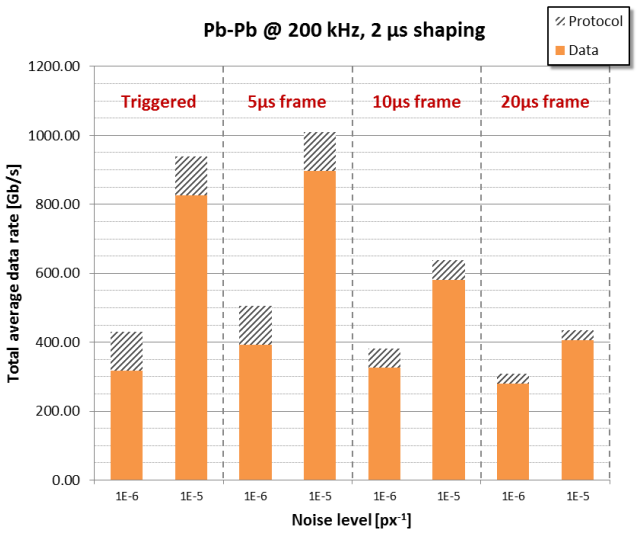

Figure 33 – Pb-Pb @ 200 kHz, 2 µs shaping.

3.5 p-p total data rates

Rates are expressed in Gbit/s for the full ITS. The orange part of the bar represents the actual hit addresses, while the pattern stripes atop shows the protocol overhead. The total required bandwidth is the sum of the two. It is foreseen to reduce the protocol overhead in the ITS Readout Electronic before sending the data to the CRU. Data are reported for a 5 µs and a 10 µs shaping time. As for the Pb-Pb graphs, values have been reported for two noise levels only, 10^{-5} and 10^{-6} px^{-1}, which represents the worst case scenario and the optimal scenario respectively. Better noise figures (< 10^{-6}) further reduce the data rate marginally, and are omitted from the graphs for clarity.

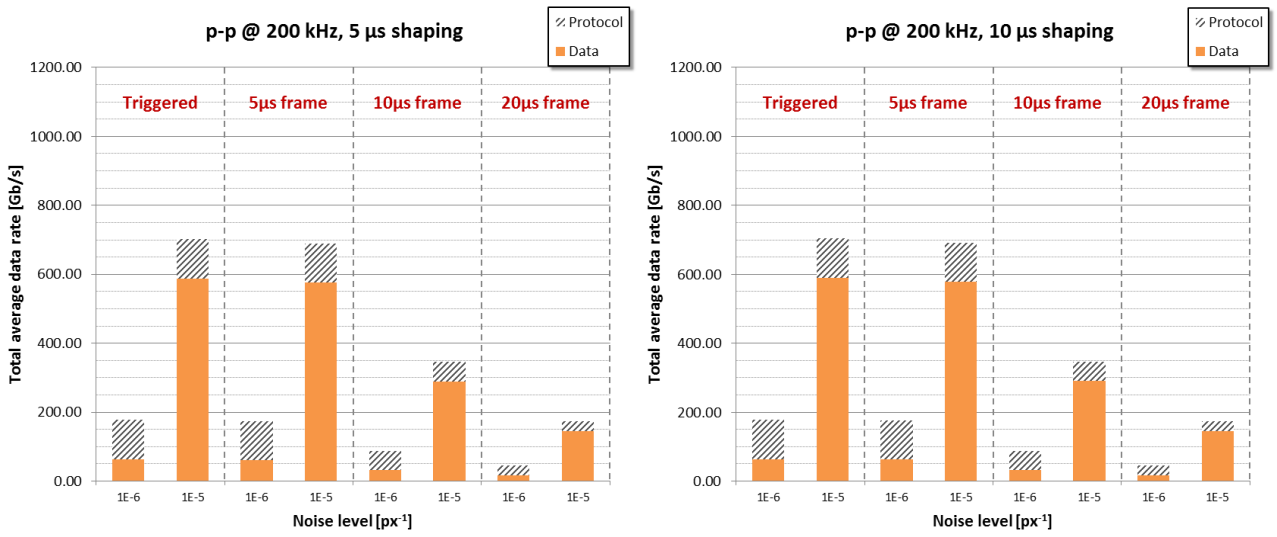

Figure 34 – p-p @ 200 kHz, 5 µs and 10 µs shaping.

In both Figure 35 and Figure 36 the data about the triggered mode are marked in red as the system cannot withstand such trigger frequencies, the resulting data throughput being not representative (data loss) of the triggered operating condition.

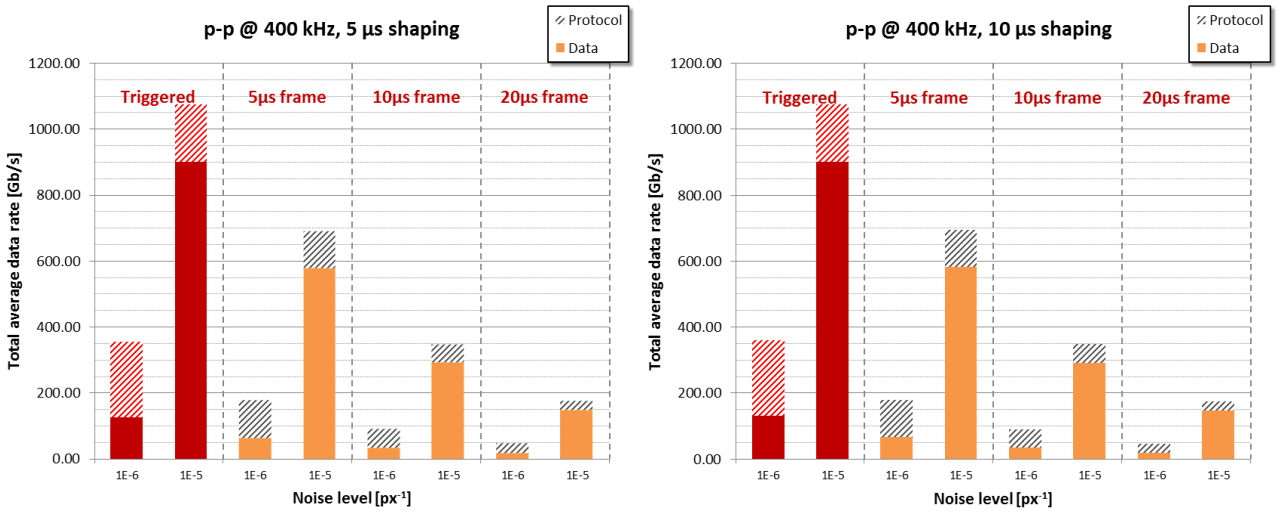

Figure 35 – p-p @ 400 kHz, 5 µs and 10 µs shaping. Trigger mode is ineffective in this scenario.

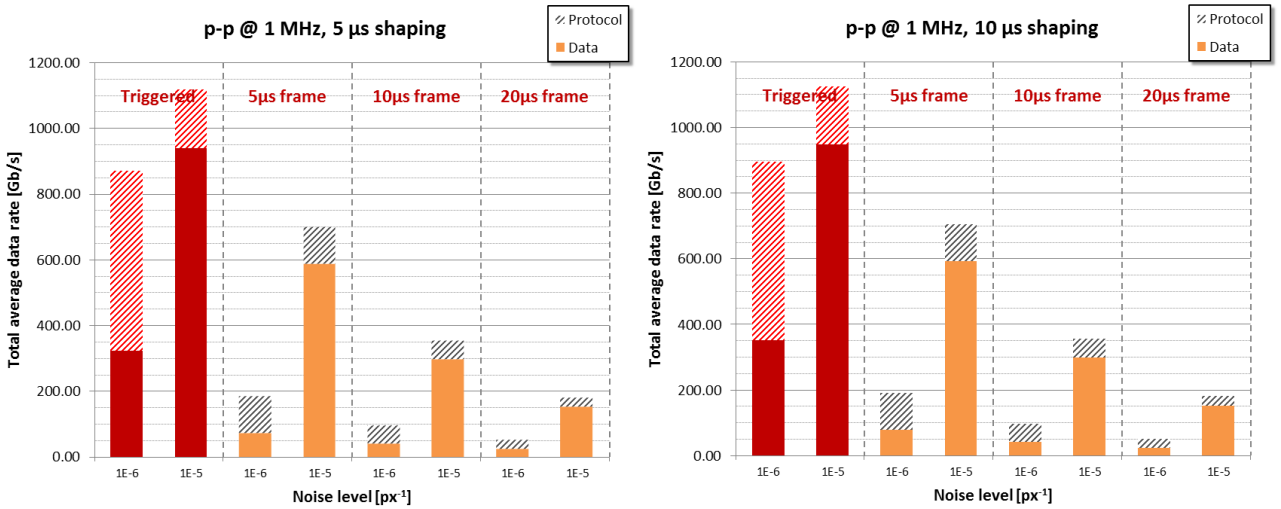

Figure 36 – p-p @ 1 MHz, 5 µs and 10 µs shaping. Trigger mode is ineffective in this scenario.

3.6 Bandwidth requirements

The data rate illustrates the average amount of data expected for the different operating conditions. The actual (maximum) bandwidth the system will have to withstand to read the ITS therefore requires a safety margin respect to those data, to account for data rate fluctuations and deviation from the foreseen operational conditions.

3.6.1 Readout Unit and maximum ratings

The ITS will be read out and controlled by a cluster of Readout Units (RUs), which will control, trigger and read each single sensor in the detector. The RUs receives control commands and delivers data directly from/to the CRU, via the CERN Versatile Link. To maximize modularity, a single RU design will serve the whole detector, the only difference between RUs attached to different layers being the input connections arrangement and the firmware parameters. The current baseline architecture for the RU is sketched in Figure 10, where only the most important connections are reported.

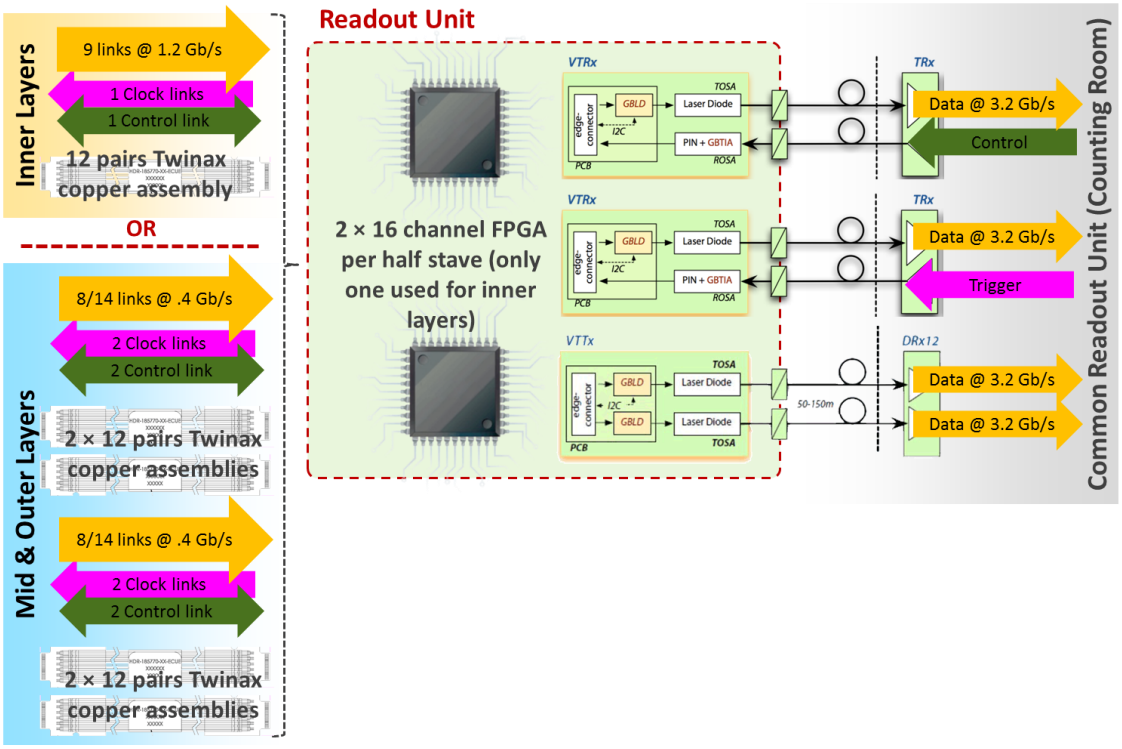

Figure 37 – Readout Unit (RU) modular implementation.

A single RU design able to serve all the layer will host three GBT links paired with two main FPGA, each one able to read up to 16 high speed links from the detector. The connection between the RU and the detector is realized with Samtec FireFly copper cables, specifically modified to be compliant with the CERN safety rules. In the foreseen configuration, in every layer one Readout Unit will read one full stave, for a total of 192 Readout Units. This arrangement ensures full modularity and a near-optimal usage of the Versatile Link payload bandwidth (3.2 Gb/s). Table 11 summarize the RUs and GBTx chipsets necessary to read out the entire ITS.

Readout Units and GBT links for maximum design rates

Layer	Staves	Copper assemblies	Copper capacity	RUs per stave	RUs per layer	VTRx count	VTTx count	Data fibers	Control fibers	Data fibers capacity	Data fibers usage
			[Gb/s]							[Gb/s]	[%]
0	12	12	103.7	1	12	24	12	36	12	115.2	90.0
1	16	16	138.2	1	16	32	16	48	16	153.6	90.0
2	20	20	172.8	1	20	40	20	60	20	192	90.0
3	24	48	122.9	1	24	48	24	48	24	153.2	80.0
4	30	60	153.6	1	30	60	30	60	30	192	80.0
5	42	168	376.3	1	42	84	42	126	42	403.2	93.3
6	48	196	430.1	1	48	96	48	144	48	460.8	93.3
Total		520	1497.6		192	384	192	576	192	1670	

Table 11 – RUs and GBTs count, distribution and usage. Note that for layer 3 & 4 only two data fibres per RU are necessary to guarantee maximum rate operations. All capacities refer to available payload.

3.6.2 Actual Bandwidth requirements

Bandwidth figures illustrated in Table 11 represent the maximum design rates of the ITS, and are necessary to obtain the maximum data rates reported in 3.2.3. Respect to the actual data rates expected for the baseline interaction rates (see 3.4 and 3.5), the design of the RUs allow for a progressive usage of the optical links, i.e. each RU can actually be connected to one, two or three GBT links depending on the foreseen usage. In the following sections, the data rate breakdown per layers clearly illustrates the effect of noise on the bandwidth usage, as well as the different number of GBTx links per unit required in each layer.

Pb-Pb interactions

Figure 38 and Figure 39 illustrate the data rate per Readout Unit (RU) for each layer for Pb-Pb interactions at 50 kHz and 100 kHz. The scale on the y axis has major steps of 3.2 Gb/s, as the payload of a single GBTx link actually is 3.2 Gb/s.

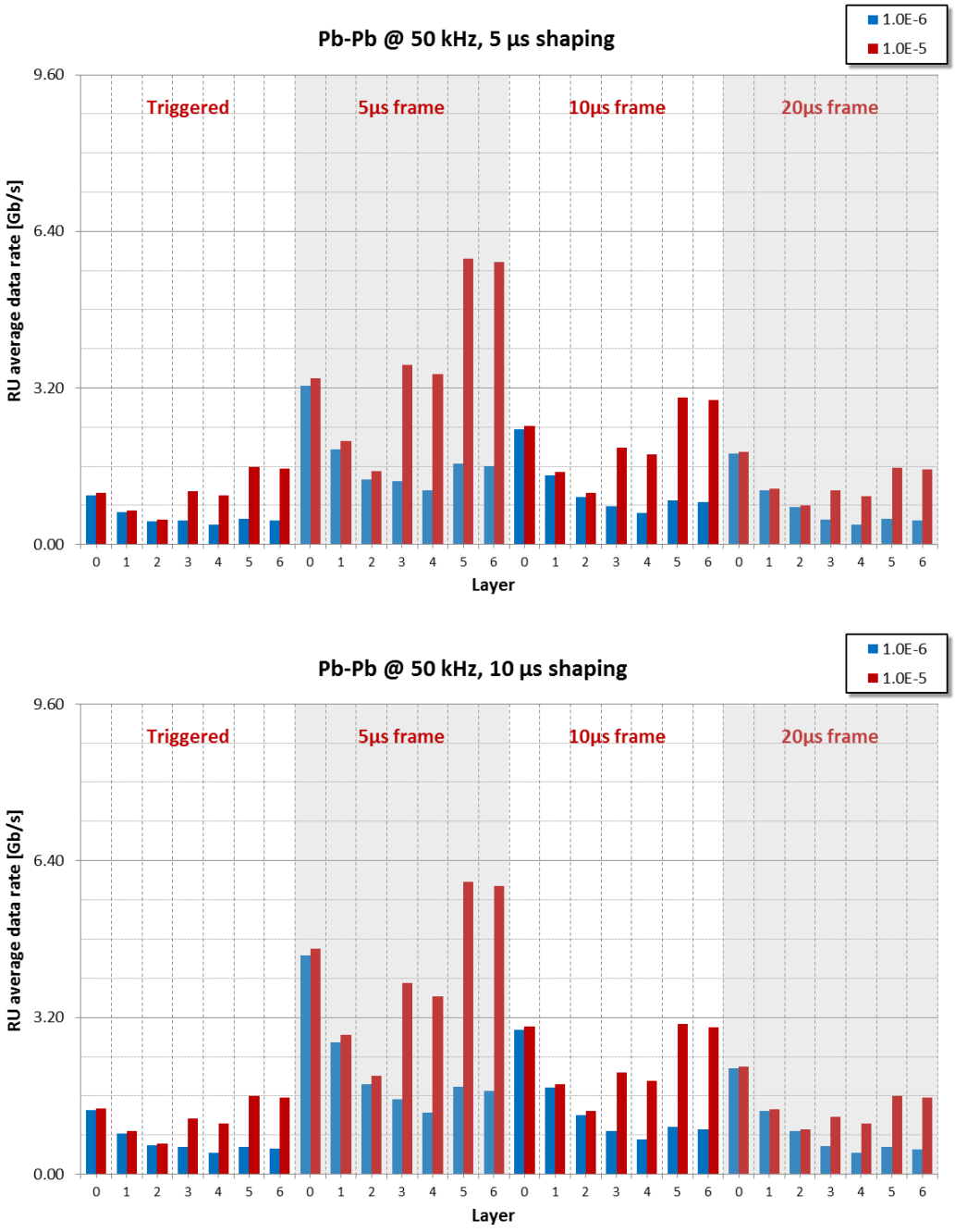

Figure 38 – Pb-Pb @ 50 kHz, 5 µs and 10 µs shaping time, total payload (data + protocol) per Readout Unit.

Pb-Pb collisions @ 50 kHz in triggered mode (baseline) are supported with one GBT link per RU all over the ITS, independently from the noise level and/or the shaping time. For this operating condition, the triggered mode is therefore the most efficient one. The same configuration can also support continuous mode with a frame length ≥ of 10 µs, at the price of much less precise time tagging of the event. Table 12 summarizes the bandwidth requirements for the different readout modes. All figures in table refer to a 10 µs shaping time, which represents the worst case option.

Data fibers and bandwidth requirements for Pb-Pb @ 50 kHz

		Triggered		Continuous 5 µs frame		Continuous 10 µs frame		Continuous 20 µs frame	
Layer	RUs	≤ 10^{-6}	≤ 10^{-5}	≤ 10^{-6}	≤ 10^{-5}	≤ 10^{-6}	≤ 10^{-5}	≤ 10^{-6}	≤ 10^{-5}
0	12	12	12	24	24	12	12	12	12
1	16	16	16	16	16	16	16	16	16
2	20	20	20	20	20	20	20	20	20
3	24	24	24	24	48	24	24	24	24
4	30	30	30	30	60	30	30	30	30
5	42	42	42	42	84	42	42	42	42
6	48	48	48	48	96	48	48	48	48
Total	192	192	192	204	348	192	192	192	192
Fiber bandwidth [Gb/s]		614.4	614.4	652.8	1113.6	614.4	614.4	614.4	614.4
Avg. bandwidth [Gb/s]		115.3	243.6	364.3	876.2	214.6	470.7	138.8	266.6

Table 12 – Data fibers count and expected bandwidth for Pb-Pb @ 50 kHz operations (assuming 10 µs shaping).

In the same fashion of Table 12 Table 13 illustrates the required number of data fibers, the maximum allocated bandwidth and the actual expected average bandwidth for Pb-Pb collisions @ 100 kHz and a shaping time of 10 µs shaping.

Data fibers and bandwidth requirements for Pb-Pb @ 100 kHz

		Triggered		Continuous 5 µs frame		Continuous 10 µs frame		Continuous 20 µs frame	
Layer	RUs	≤ 10^{-6}	≤ 10^{-5}	≤ 10^{-6}	≤ 10^{-5}	≤ 10^{-6}	≤ 10^{-5}	≤ 10^{-6}	≤ 10^{-5}
0	12	24	24	36	36	24	24	24	24
1	16	16	16	32	32	32	32	16	16
2	20	20	20	20	20	20	20	20	20
3	24	24	24	24	48	24	24	24	24
4	30	30	30	30	60	30	30	30	30
5	42	42	84	42	84	42	84	42	42
6	48	48	96	48	96	48	96	48	48
Total	192	204	294	232	376	220	310	204	204
Fiber bandwidth [Gb/s]		652.8	940.8	742.4	1203.2	704	992	652.8	652.8
Avg. bandwidth [Gb/s]		291.2	546.6	511.8	1015.0	338.0	592.5	228.4	355.2

Table 13 – Data fibers count & expected bandwidth for Pb-Pb @ 100 kHz operations (10 µs shaping).

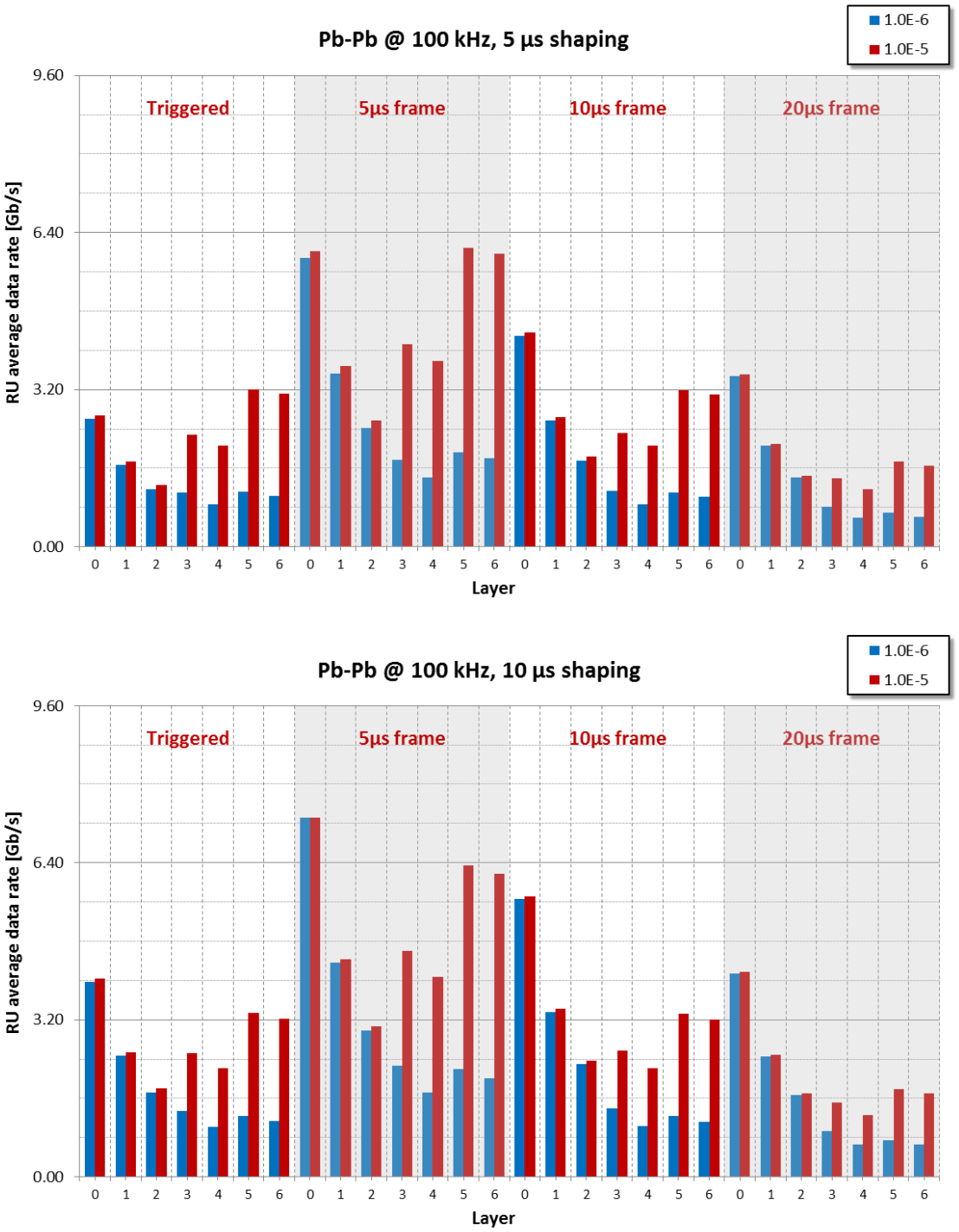

Figure 39 – Pb-Pb @ 100 kHz, 5 µs and 10 µs shaping time, total payload (data + protocol) per Readout Unit.

Pb-Pb collisions @ 200 kHz in both triggered and continuous mode (Figure 40) data rates are reported as reference for future upgrades, for shaping times of 2 µs and 5 µs only (10 µs data available). Table 14 reports the number of required fibers and the expected average bandwidth values for such hypothetical condition.

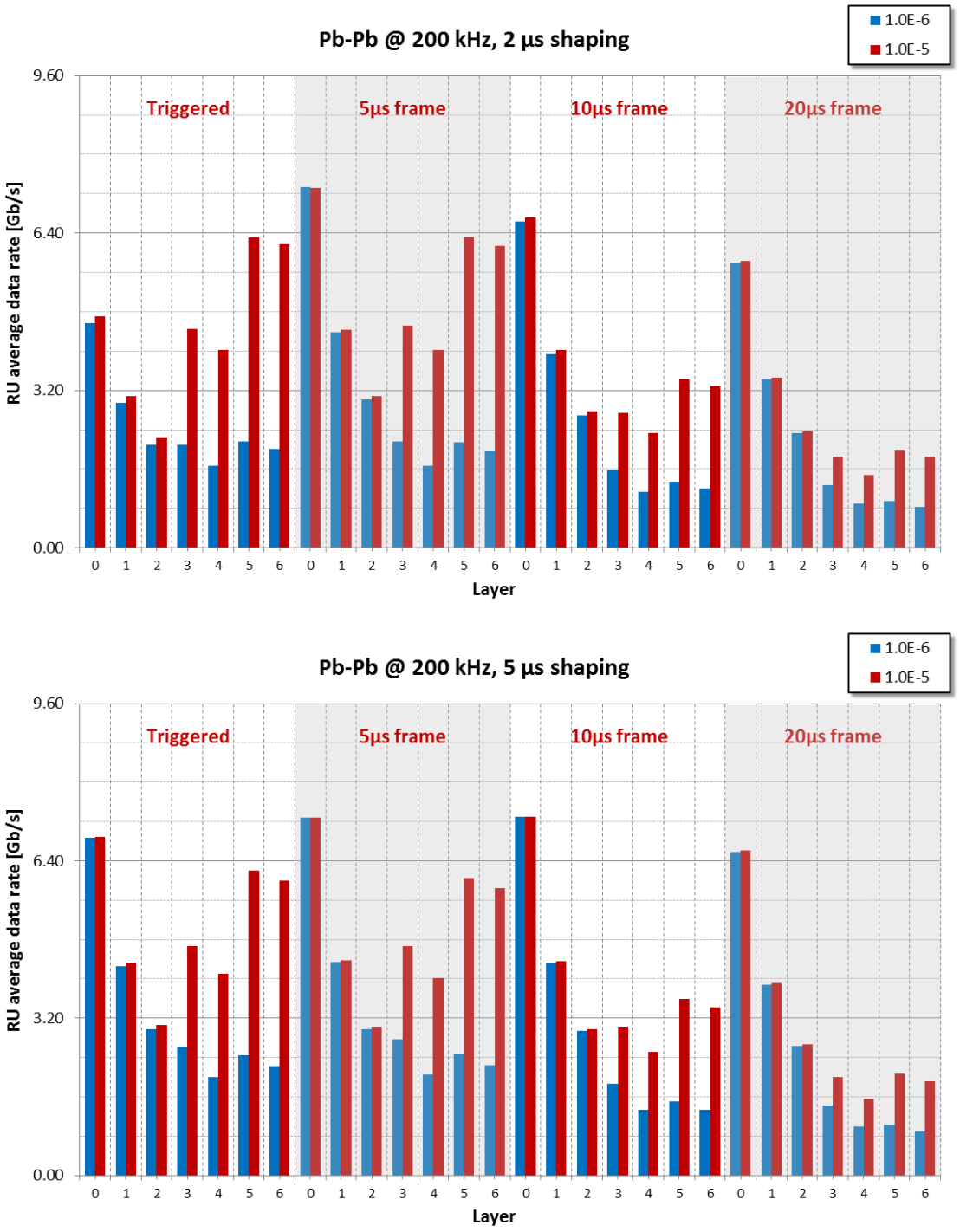

Figure 40 – Pb-Pb @ 200 kHz, 2 µs and 5 µs shaping time, total payload (data + protocol) per Readout Unit.

Data fibers and bandwidth requirements for Pb-Pb @ 200 kHz

		Triggered		Continuous 5 µs frame		Continuous 10 µs frame		Continuous 20 µs frame	
Layer	RU count	≤ 10^{-6}	≤ 10^{-5}	≤ 10^{-6}	≤ 10^{-5}	≤ 10^{-6}	≤ 10^{-5}	≤ 10^{-6}	≤ 10^{-5}
0	12	36	36	36	36	36	36	36	36
1	16	32	32	32	32	32	32	32	32
2	20	20	20	20	20	20	20	20	20
3	24	48	48	48	48	24	48	24	24
4	30	30	60	30	60	30	30	30	30
5	42	42	84	42	84	42	84	42	42
6	48	48	96	48	96	48	96	48	48
Total	192	256	376	256	376	232	346	232	232
Fiber bandwidth [Gb/s]		819.2	1203.2	819.2	1203.2	742.4	1107.2	742.4	742.4
Avg. bandwidth [Gb/s]		634.7	932.0	639.3	916.8	469.1	719.3	384.4	508.6

Table 14 – Data fibers count & expected bandwidth for Pb-Pb @ 200 kHz operations (10 µs shaping).

p-p interactions

Figure 41 and Figure 42 illustrate the data rate per RU for each layer for p-p interactions at 200 kHz and 400 kHz for both 5 µs and 10 µs shaping time. Noise is the dominant factor in determining the necessary bandwidth for protons. For interaction frequencies higher than 200 kHz, the most effective way of reading out the ITS for p-p events is using the continuous mode. Already at 400 kHz the triggered mode leads to significant data loss.

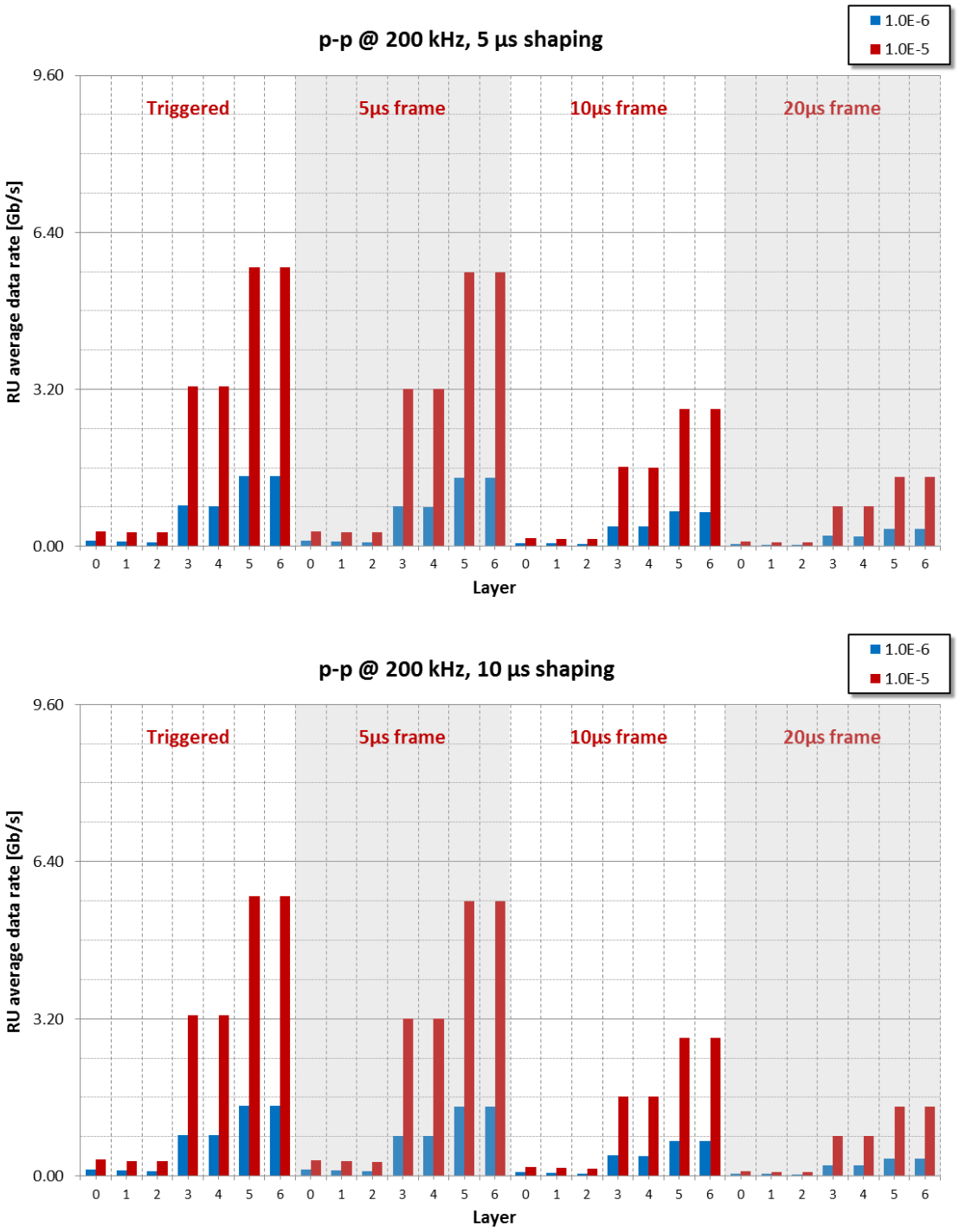

Figure 41 – p-p @ 200 kHz, 5 µs and 10 µs shaping time, total payload (data + protocol) per Readout Unit.

p-p collisions @ 200 kHz in triggered mode (baseline) can be supported with one GBTx link per RU all over the ITS (165 GBT links in total) if the noise is equal or better than 1×10^{-6}, and the same holds for continuous operations with 5 µs frame length. In case the noise is up to 1×10^{-5}, 1 links per RU will suffice for the 1st, 2nd and 3rd layer, three links per RU will be necessary for the 4th and 5th layers, and 2 links per RU for the 6th and 7th layers. Total required links and bandwidth are summarized in **Error! Reference source not found.** for the ifferent noise and operating conditions.

Data fibers and bandwidth requirements for p-p @ 200 kHz

		Triggered		Continuous 5 μs frame		Continuous 10 μs frame		Continuous 20 μs frame	
Layer	RU count	≤ 10^{-6}	≤ 10^{-5}	≤ 10^{-6}	≤ 10^{-5}	≤ 10^{-6}	≤ 10^{-5}	≤ 10^{-6}	≤ 10^{-5}
0	12	12	12	12	12	12	12	12	12
1	16	16	16	16	16	16	16	16	16
2	20	20	20	20	20	20	20	20	20
3	24	24	48	24	48	24	24	24	24
4	30	30	60	30	60	30	30	30	30
5	42	42	84	42	84	42	42	42	42
6	48	48	96	48	96	48	48	48	48
Total	192	192	336	192	336	192	192	192	192
Fiber bandwidth [Gb/s]		614.4	1075.2	614.4	1075.2	614.4	614.4	614.4	614.4
Avg. bandwidth [Gb/s]		115.3	243.6	364.3	876.2	214.6	470.7	138.8	266.6

Table 15 – Data fibers count & expected bandwidth for p-p @ 200 kHz operations (10 μs shaping).

p-p collisions @ 400 kHz in triggered mode cannot be supported without some data loss occurring in the Middle and Outer Layers if the noise level is 1×10^{-5}, even if the Inner layers show no problems. Data reported in **Error! Reference source not found.** therefore assume some data loss will happen in the Middle and Outer ayers in triggered mode. For noise levels equal or better than 1×10^{-5}, 400 kHz triggered operation are possible and require a total of 309 GBT links to be connected to the ITS. In continuous mode, 5 μs frame length requires 309 GBT links in case of 1×10^{-5}noise, and 165 GBT ling for noise levels equal or better than 1×10^{-6}.

Data fibers and bandwidth requirements for p-p @ 400 kHz

		Triggered		Continuous 5 μs frame		Continuous 10 μs frame		Continuous 20 μs frame	
Layer	RU count	≤ 10^{-6}	≤ 10^{-5}	≤ 10^{-6}	≤ 10^{-5}	≤ 10^{-6}	≤ 10^{-5}	≤ 10^{-6}	≤ 10^{-5}
0	12	12	12	12	12	12	12	12	12
1	16	16	16	16	16	16	16	16	16
2	20	20	20	20	20	20	20	20	20
3	24	24	48	24	48	24	24	24	24
4	30	30	60	30	60	30	30	30	30
5	42	42	126	42	84	42	42	42	42
6	48	48	144	48	96	48	48	48	48
Total	192	192	426	192	336	192	192	192	192
Fiber bandwidth [Gb/s]		614.4	1363.2	614.4	1075.2	614.4	614.4	614.4	614.4
Avg. bandwidth [Gb/s]		291.2	546.6	511.8	1015.0	338.0	592.5	228.4	355.2

Table 16 – Data fibers count & expected bandwidth for p-p @ 400 kHz operations (10 μs shaping).

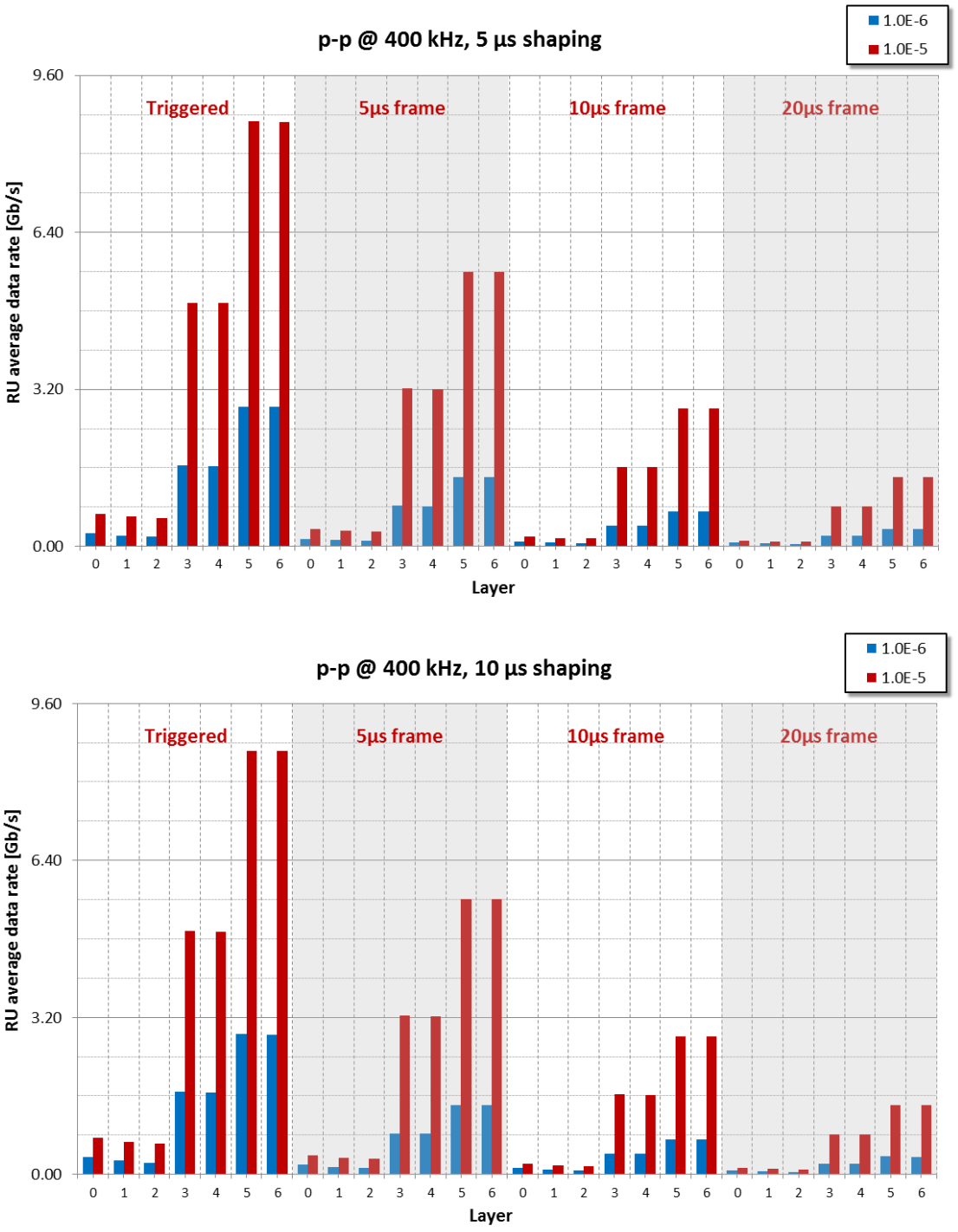

Figure 42 – p-p @ 400 kHz, 5 µs and 10 µs shaping time, total payload (data + protocol) per Readout Unit.

p-p collisions @ 1 MHz in both triggered and continuous mode data rates are also reported as reference for future upgrades (Figure 43).

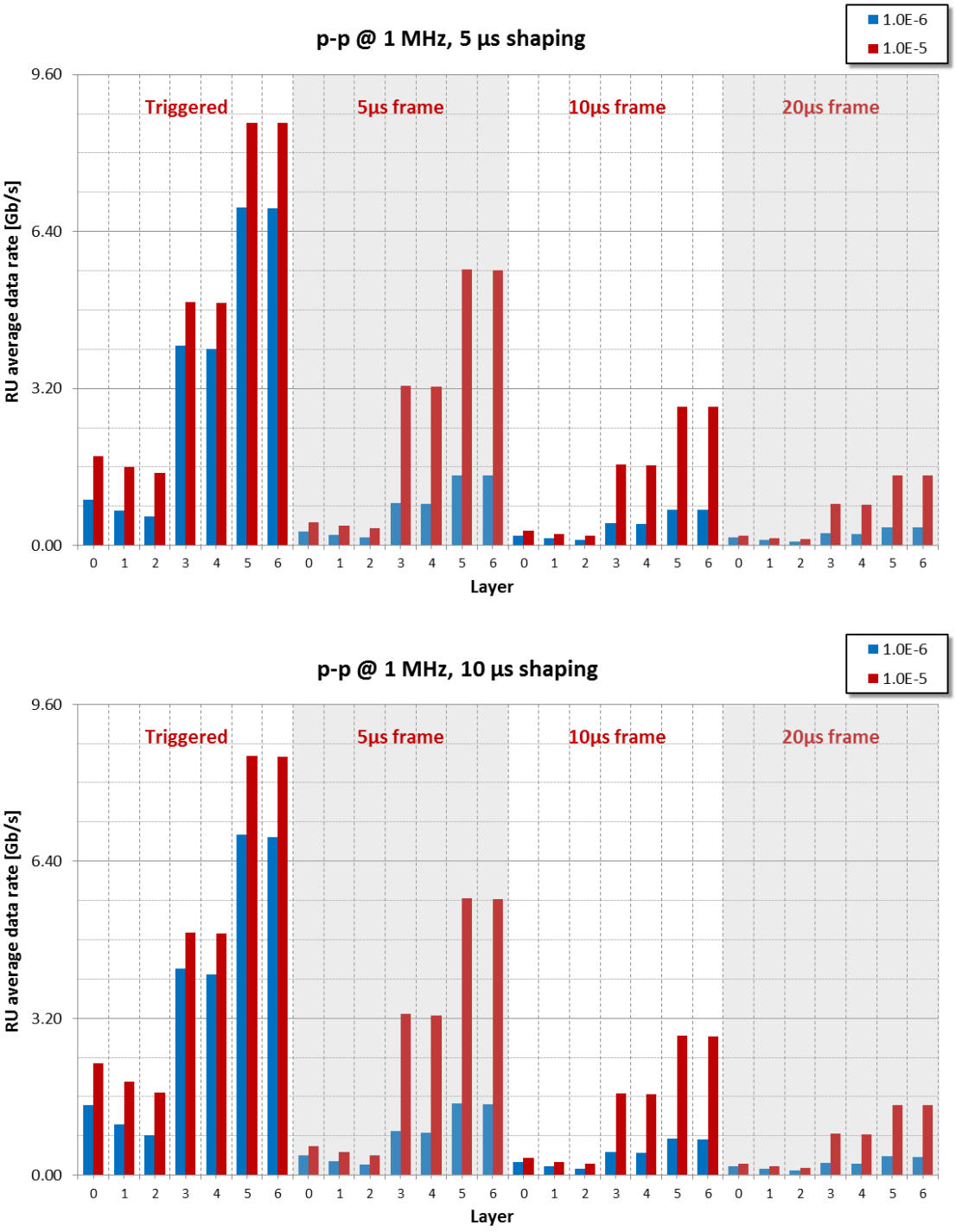

Figure 43 – p-p @ 1 MHz, 5 µs and 10 µs shaping time, total payload (data + protocol) per Readout Unit.

Data fibers and bandwidth requirements for p-p @ 1 MHz

		Triggered		Continuous 5 µs frame		Continuous 10 µs frame		Continuous 20 µs frame	
Layer	RU count	≤ 10^{-6}	≤ 10^{-5}	≤ 10^{-6}	≤ 10^{-5}	≤ 10^{-6}	≤ 10^{-5}	≤ 10^{-6}	≤ 10^{-5}
0	12	12	12	12	12	12	12	12	12
1	16	16	16	16	16	16	16	16	16
2	20	20	20	20	20	20	20	20	20
3	24	48	48	24	48	24	24	24	24
4	30	60	60	30	60	30	30	30	30
5	42	126	126	42	84	42	42	42	42
6	48	144	144	48	96	48	48	48	48
Total	192	426	426	192	336	192	192	192	192
Fiber bandwidth [Gb/s]		1363.2	1363.2	614.4	1075.2	614.4	614.4	614.4	614.4
Avg. bandwidth [Gb/s]		634.7	932.0	639.3	916.8	469.1	719.3	384.4	508.6

Table 17 – Data fibers count & expected bandwidth for p-p @ 1 MHz operations (10 µs shaping).

3.6.3 Summary

The readout Electronic is being designed to exploit the full ITS capacity, i.e. to read it at the maximum possible speed, which is ultimately set by the sensor architecture and the available bandwidth between the ITS and the Readout Electronic itself. To ensure the possibility to read the ITS at maximum speed, it is foreseen to lay down all the necessary optical links between the Readout Electronic and the CRU/O2 system, as detailed in Table 11 in 3.6.1. Table 18 below is a short recall of Table 11, and highlights that the total number of physical links going to be installed will therefore be 522 (3 data links for each Readout Unit in layers 0, 1, 2, 5, 6 and data 2 links for each Readout Unit in layers 3 and 4).

Readout electronic deployment

Layer	Staves	RU count	Data fibers	Control fibers	Trigger fibers
0	12	12	36	12	12
1	16	16	48	16	16
2	20	20	60	20	20
3	24	24	48	24	24
4	30	30	60	30	30
5	42	42	126	42	42
6	48	48	144	48	48
Total		192	522	192	192

Table 18 – Summary of the Readout Unit and GBT links (data, trigger and control) foreseen for installation.

While the number of installed links is fixed, the number of links actually used to transmit data will vary accordingly to the operational mode of the ITS: Table 19 reports the number of links foreseen necessary to read the ITS in the different operating modes. The RUs will use the redundant links as spares in case of link malfunctions in all those modes where less than 3 link per RU are necessary.

GBT data active fibers (fibers actually transmitting data) and equivalent maximum/average bandwidth

		Triggered		5 µs frame		10 µs frame		20 µs frame	
Noise [px^{-1}]		10^{-6}	10^{-5}	10^{-6}	10^{-5}	10^{-6}	10^{-5}	10^{-6}	10^{-5}
Pb-Pb @ 50 kHz	Fibers	48	48	48	96	48	48	48	48
	Capacity Average	614 <115>	614 <244>	653 <364>	1114 <876>	614 <215>	614 <471>	614 <139>	614 <267>
Pb-Pb @ 100 kHz	Fibers	204	294	232	376	220	310	204	204
	Bdwt. <Avg>	653 <291>	941 <547>	742 <512>	1203 <1015>	704 <338>	992 <593>	653 <228>	653 <355>
Pb-Pb @ 200 kHz	Fibers	256	376	256	376	232	346	232	232
	Bdwt. <Avg>	819 <635>	1203 <932>	819 <639>	1203 <917>	742 <469>	1107 <719>	742 <384>	742 <509>
p-p @ 200 kHz	Fibers	192	336	192	336	192	192	192	192
	Bdwt. <Avg>	614 <115>	1075 <244>	614 <364>	1075 <876>	614 <215>	614 <471>	614 <139>	614 <267>
p-p @ 400 kHz	Fibers	192	426	192	336	192	192	192	192
	Bdwt. <Avg>	614 <291>	1363 <547>	614 <512>	1075 <1015>	614 <338>	614 <593>	614 <228>	614 <355>
p-p @ 1 MHz	Fibers	426	426	192	336	192	192	192	192
	Bdwt. <Avg>	1363 <635>	1363 <932>	614 <639>	1075 <917>	614 <469>	614 <719>	614 <384>	614 <509>

Table 19 – Actual data fibers required (top number for each condition), equivalent maximum bandwidth in Mb/s (bottom number) and expected actual average bandwidth in Mb/s (between brackets).

Figures reported in Table 19 assumes a raw data flow from the Readout Units, without any further data reduction/compression nor any data sparsification applied. Due to the fact that the majority of the GBT links will not operate at full bandwidth (3.2 Gb/s), the actual average data rate from the ITS will be less than what reported in Table 19, which represents a maximum upper limits. The greyed boxes are operational modes not supported by the present ITS implementation (they could become available depending on Readout Electronic development and user requirements).

Figure 44 and Figure 45 summarize the total data rate expected for the same operational conditions of Table 19. The reported figures therefore represent the actual average data load the CRU/O2 system will have to deal with. The figures for p-p @ 400 kHz in triggered mode are patterned because the system is not fully efficient at such trigger rates.

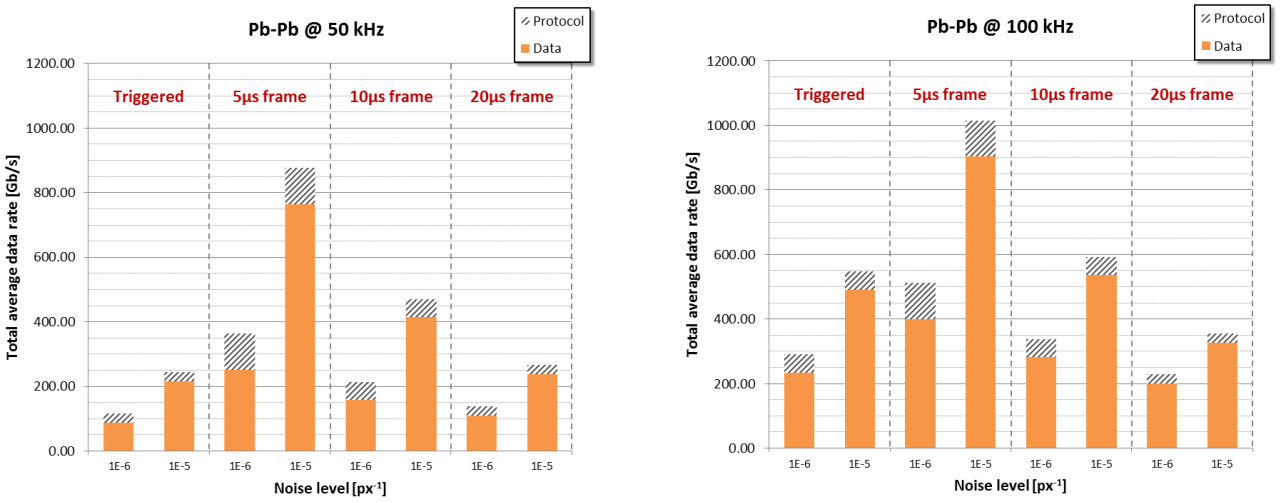

Figure 44 – Pb-Pb total data rates in Gb/s.

Some data rate reduction could be obtained by further optimizing the protocol inside the Readout Units. The present protocol has been in fact optimized for the baseline operation mode (Pb-Pb @ 50 or 100 kHz)

and trying to simplify as much as possible its in-chip implementation to spare chip resources. There is therefore some margin, especially for p-p interactions, to further reduce the protocol overhead, even if a 20-30% reduction of the protocol overhead would not drastically change the situation, especially in case of noise levels of 1×10^{-5}. To reduce the data flow of a relevant factor (two or more), some sort of tracking information has to be used/produced in order to only pass those hits which actually belongs to real tracks.

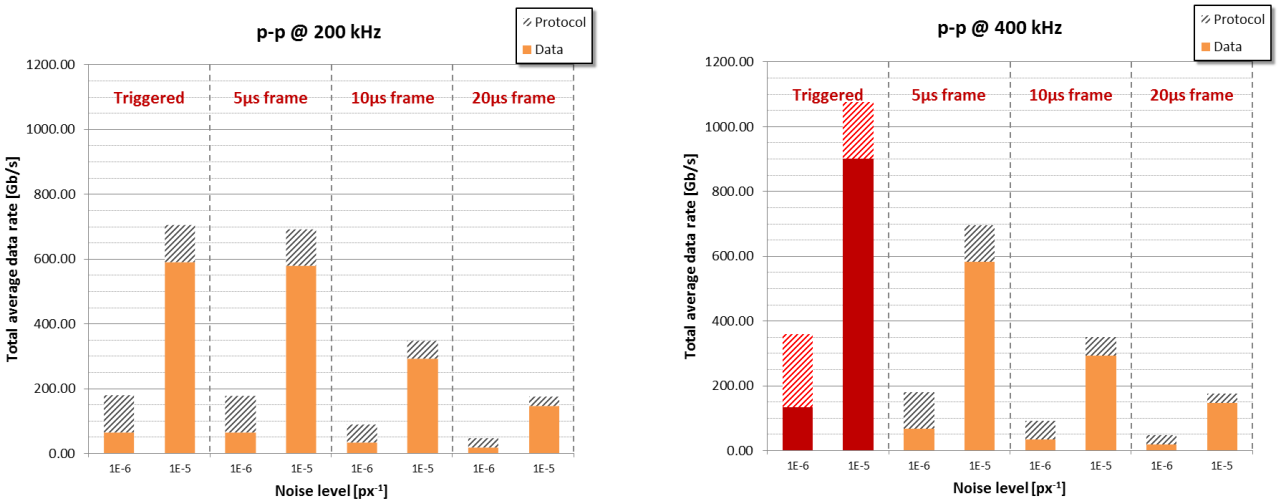

Figure 45 – p-p total data rates in Gb/s (in red not-supported modes).

4 System implementation

This section analyses the different options and solutions adopted to build the Readout Electronic system, based on previous sections findings.

4.1 Stave buses & copper links

4.1.1 Bus

The chips are connected to the Readout Unit by the stave bus the copper links 1.1.3. The copper links performance have been evaluated using available commercial samples, while for the stave bus, which is in R&D phase, models and mock-ups have been used. In particular, the behaviour of the bus for different properties of the strips (material, roughness, thickness, spacing, etc.) have been explored through models to check the consistency with the real measurements. Four main elements have been highlighted:

- Resistivity of the bulk material
- Effective resistivity of the metal laminate
- Skin depth
- Roughness of surface traces

4.1.2 Copper links

The copper links which will be employed are a custom made version (to comply with safety rules) of the Samtek AWG30 twinax, which could actually employ AEG32 conductors if testing will prove they can meet the specification. So far, all testing has been performed with the AWG30 twinax (Figure 46).

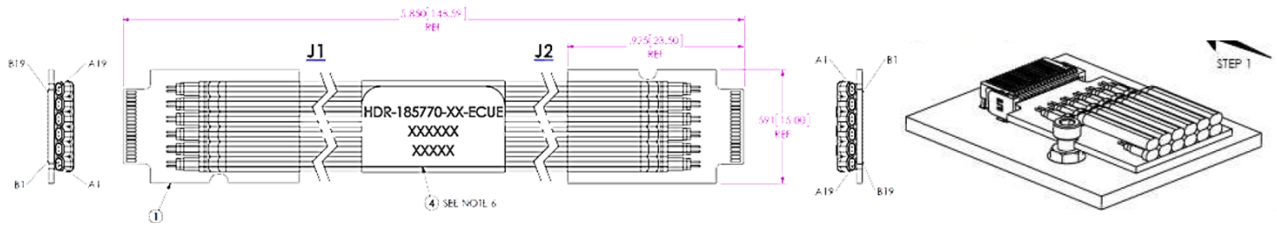

Figure 46 – Samtec custom-made cable assembly.

The custom-made variant of the cable will use different dielectric and cladding (both halogen free), and will therefore have different mechanical properties (yet to be determined). The electrical properties will stay unchanged (or improved) respect to the commercial version of the cable. Table 20 summarizes the electrical characteristic the final cable will comply with.

Parameter	Reference value
Impedance	100 Ω ± 5%
Insertion loss	< 0.3 dB/m @ 1 GHz
Return loss	-30 dB @ 1 GHz for a 10 m cable
Within pair skew	< 2.5 – 5.0 ps/m
Pair to pair skew	< 50 ps/m
Capacitance	Up to the designers

Table 20 – Copper cables electrical specifications.

Samples of the custom cables has been neutron-irradiated to check halogen contents. The cable was first disassembled into five layers L1–L5, detailed in Table 21. After irradiation, it was possible to measure the quantity of relevant halogens in L1 and L4 (cladding and dielectric).

Layer	Material	Mass
		[mg]
L1	Polyolefine Megolon S-344	142.80
L2	Silver plated copper	NA
L3	Copper	NA
L4	Low density PE	115.41
L5	Copper	NA

Table 21 – Custom cable layers

Table 22 shows the elements content found in the Samtec custo cable.

Sample	Cl	Br	I	Al	S
	[mg kg-1]	[mg kg-1]	[mg kg-1]	[%]	[%]
L1	9.95 ± 1.5	< 0.8	< 0.3	18.1± 1.0	< 0.07
L4	224 ± 2.0	< 0.3	< 0.1	< 0.075	< 0.04

Table 22 – Halogen contents in L1 and L4

Polymer layers L1 and L4 of cable SAMTEC satisfy the requirements on the halogen and sulfur contents, if we consider the older specification [##] that the value < 0.1 % means “halogen and sulfur free”. It can be concluded that both polymer layers L1 and L4 of Samtec custom cable have low contents of Cl, Br, I and sulfur. Thus the individual polymers may be considered to satisfy the requirements of the CERN Internal Safety Note Nr. 23 [##] and the CERN Internal Safety note Nr. 41 [##].

4.1.3 Bus – copper links mock-up measurements

Eye-Height	pre-emphasis			
MHz	00 no	01 low	10 mid	11 high
40	541	492	588	602
160	460	491	568	545
250	410	413	571	550
320	362	390	535	570
500	300	445	494	520
750	200	452	530	445
1000	145	363	575	487
1500	67	240	445	552
2000	28	183	410	500
2500		166	250	400

Q-factor	pre-emphasis			
MHz	00 no	01 low	10 mid	11 high
40	23,5	23	24,5	24,8
160	14,5	21	24	19
250	10,9	8,9	20,3	20,9
320	9,2	8	13	22
500	7,2	10,7	9,6	11,4
750	5,2	12,8	11,9	7,6
1000	4,4	8,1	17,1	8,9
1500	3,6	5,3	9	13
2000	3,2	4,6	7	11,5
2500		4	5,2	7,8

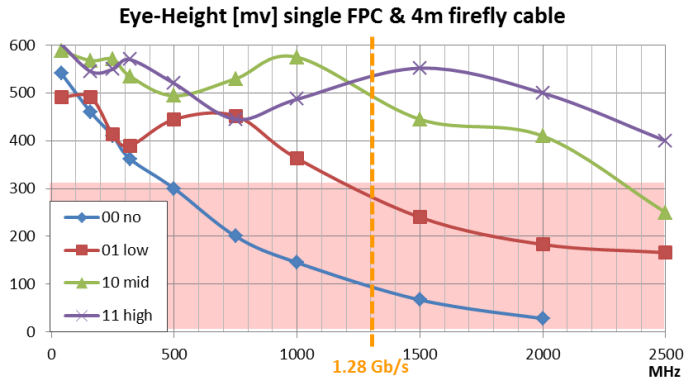

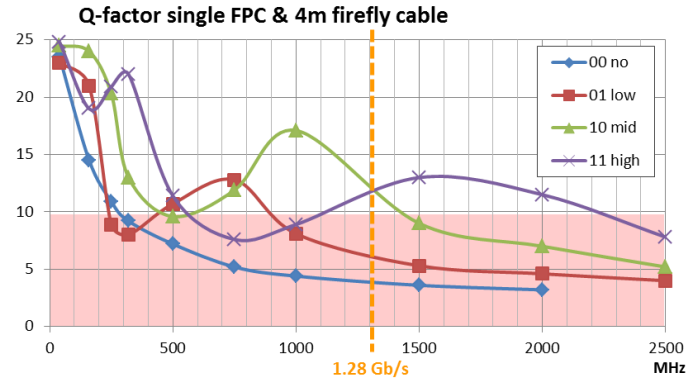

Figure 47 – Inner Layers configuration test mock-up measurements. 30 cm long FPC plus 4m AWG30 twinax cables.

Eye-Height	pre-emphasis			
MHz	00 no	01 low	10 mid	11 high
40	432	400	471	479
160	320	395	424	398
250	220	383	415	354
320	186	366	395	350
500	50	285	346	335
750		119	190	207
1000			56	107
1500				
2000				
2500				

Q-factor	pre-emphasis			
MHz	00 no	01 low	10 mid	11 high
40	18	18,6	18,6	18,2
160	9,5	19,5	15,1	11,9
250	6,1	16,8	15,6	10,2
320	5,5	14,5	13,2	10,3
500	3,5	8,8	10,1	9,6
750	2,6	4,4	5,2	5,5
1000	1,9	2,9	3,5	4,1
1500				
2000				
2500				

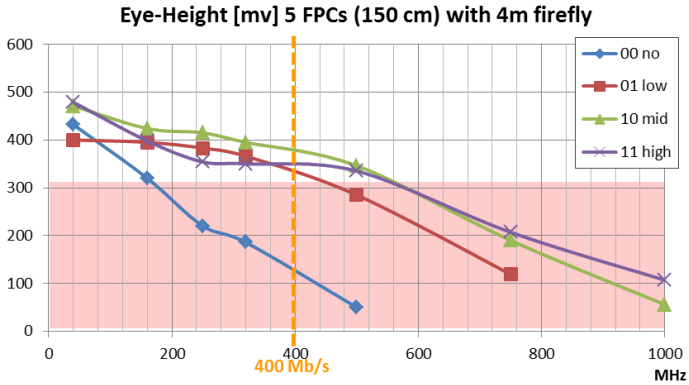

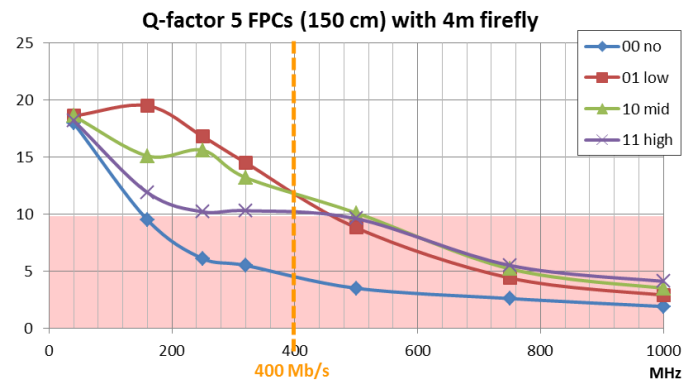

Figure 48 – Middle/Outer Layers configuration test mock-up measurements. 150 cm long FPC plus 4m AWG30 twinax cables.

4.1.4 Prototype copper links measurements

Prototypes cables from SAMTEC have been tested to check their actual performance.

4.2 Readout Unit

The ALICE ITS Readout Electronic is composed by modular Readout Units (RU), each one responsible of controlling and retrieving data from one stave. 192 RUs will form the readout and control system of the full ITS. Table 23 is a copy of Table 2 placed here to provide a quick reference of the RUs connections. The RU has been designed to exploit the available CERN Versatile Link as hardware control and data connection layer to the counting room, hence Table 23 reports the quantities of Versatile Link components necessary to build the system.

Readout Units and optical components for maximum design rates

Layer	Staves	Copper assemblies	Copper capacity	RUs per stave	RUs per layer	VTRx count	VTTx count	Data fibers	Control fibers	Data fibers capacity	Data fibers usage
			[Gb/s]							[Gb/s]	[%]
0	12	12	103.7	1	12	24	12	36	12	115.2	90.0
1	16	16	138.2	1	16	32	16	48	16	153.6	90.0
2	20	20	172.8	1	20	40	20	60	20	192	90.0
3	24	48	122.9	1	24	48	24	48	24	153.2	80.0
4	30	60	153.6	1	30	60	30	60	30	192	80.0
5	42	168	376.3	1	42	84	42	126	42	403.2	93.3
6	48	196	430.1	1	48	96	48	144	48	460.8	93.3
Total		520	1497.6		192	384	192	576	192	1670	

Table 23 – RUs and VTRx/VTTx count, distribution and usage. Note that for layer 3 & 4 only two data fibres per RU are necessary to guarantee maximum rate operations. All values refer to available payload.

4.2.1 CERN Versatile Link

The Versatile Link is a custom-made optical link system designed to carry data, triggering and slow control signal in radiation environments over a single, bi-directional optical link (Figure 49) [GBT]. The electronic component hosted in the cavern side of the link has been specially designed at CERN to operate in high-radiation environment, ensuring resistance to both total dose and single event effects. The counting room side electronic relies instead on commercial COTS; FPGA hardware language blocks implementing the protocol necessary to communicate through the link are available from CERN [GTB FPGA].

The ITS readout electronic connect directly to the GBTx chip [GBTx] through its e-link interfaces, a programmable set of bi-directional data and clock lines. Each e-link comprises three links: a transmit line, a receive line, and a dedicated clock line (Figure 50). A single GBTx chip handles up to 40 e-links on the front-end side and a bidirectional optical link toward the counting room.

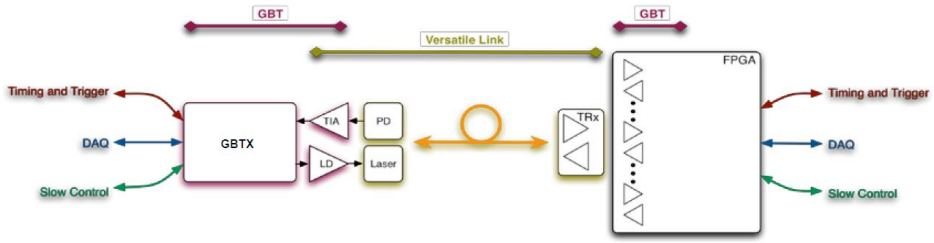

Figure 49 – GBT link schematic, cavern on the left, counting room on the right.

The total optical link capacity for the user is 3.2 Gb/s of data, which can be re-routed to different e-links on the user side, up to a maximum of 320 Mb/s per e-link. All figures refer to the available payload data rate, while the actual capacity of the link, 4.2 Gb/s, is used for link management and error correction redundancy. While it is possible to operate the GBT without its own protocols to access the full bandwidth, this is not the case for the ITS readout electronic.

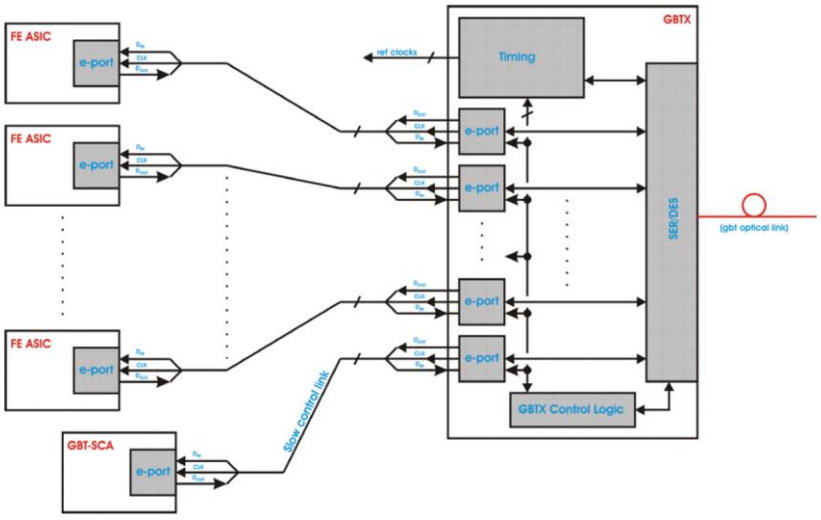

Figure 50 – GBTx chip (front end custom-made chip) connections.

E-link can be grouped in different fashion and speeds, yet for the readout of the ITS it is foreseen to operate them at the maximum available speed of 320 Mb/s, yielding a total of 10 e-links available per each GBTx chip. In the present configuration, each RU will incorporate 3 GBTx chips to manage one downlink from the counting room, 3 uplink to the counting room (even if only one will be used at the beginning, see 3.6.2) and a dedicated ling to receive the trigger. One available link is left for possible future expansion.

4.2.2 Readout Unit to GBT links routing

Given the 1:1 pairing between the RUs and the staves, and that all the RU have identical hardware, data routing from sensors to the counting room is organized in different ways accordingly to the layers group. Figure 51 illustrates the hardwiring between the GBTx chip and the optical transceivers mounted on the RU. One GBTx chip is used to drive a VTRx optical transceiver, with one data uplink to the counting room (orange arrow) and one control downlink from the counting room (green arrow). As a single GBT chip can handle only one uplink connection, two GBT chips are used to drive the VTTx optical transmitter, which drives two separate fibres channel (two orange arrows). The third GBT chip is also used to receive the trigger data from a separate VTRx transceiver. While the VTRx and VTTx modules tasked to transmit the data stream are Multi Mode (MM) ones, the VTRx transceiver receiving the trigger is a Single Mode (SM) one, which is the default way of transmitting the trigger optically among the LHC experiments. In picture two FPGAs of different kind are present, but this is just a placeholder for a programmable devices section, as no final decision on which exact configuration has been made yet.

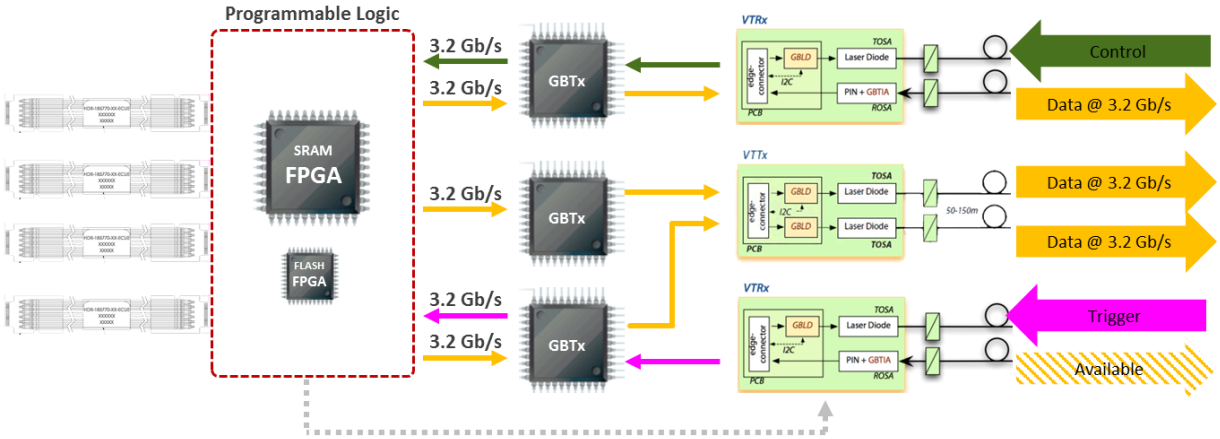

Figure 51 – Hardwired connection between GBTx chip and optical transceivers in the RU.

4.2.3 Sensor to GBT data and control routing

Considering the connections of Figure 51, 3 different data path between the sensor and the GBT chips are used by the programmable logic accordingly to which layer the RU is connected. In the following schematics, two FPGAs per readout unit represent the programmable logic, but the topology is actually independent from the actual number of physical devices used, which will depend on the final implementation of the architecture. Figure 52 illustrate the Inner Layers connection. It is worth remembering that for baseline operations (50 kHz Pb-Pb) a single GBTx chip will provide enough bandwidth (see 3.6.2), and the other could be used to hot-swap fibre lines in case of connection problems. To connect to the Innermost Layers staves, only the first connector (A) is used, with the clock and control lines and 9 data lines running over the 12 available links.

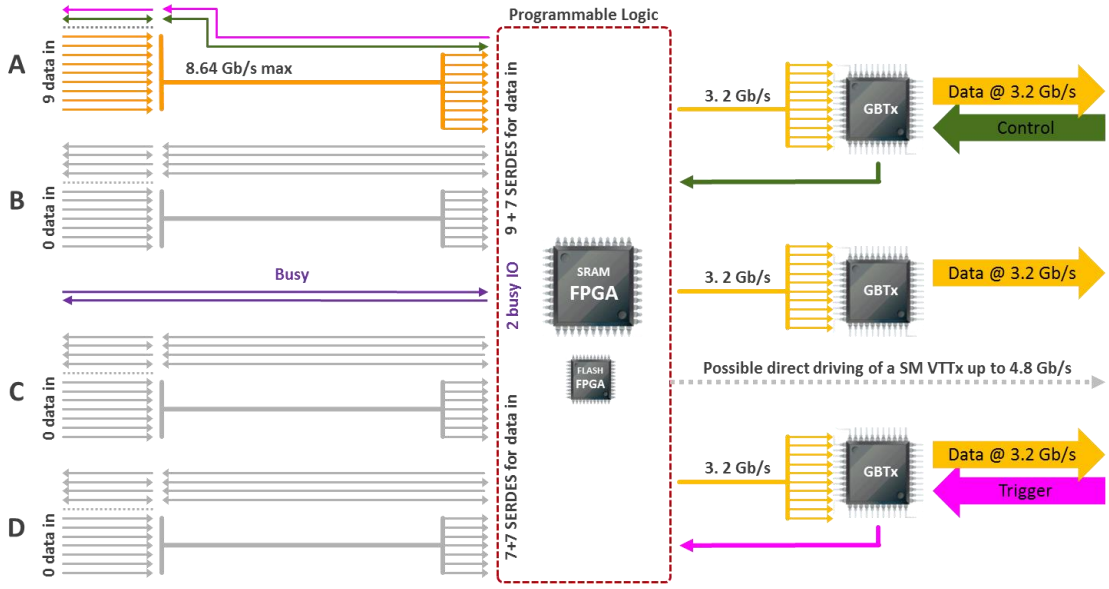

Figure 52 – **Inner Layers** data and controls routing schematic.

Figure 53 illustrates the Middle Layers connection. In such configuration all 4 connectors are used, with identical signal routing. While the clock and control lines are identical for all 4 connectors, the data lines are reduced to 7 in connectors B, C and D to make room for one additional clock and control links pair which will be used in the MFT readout. This distinction is relevant only in case hardware SERDES are employed; in case fabric IO pins can provide the required speed, the connection constrains will be greatly reduced.

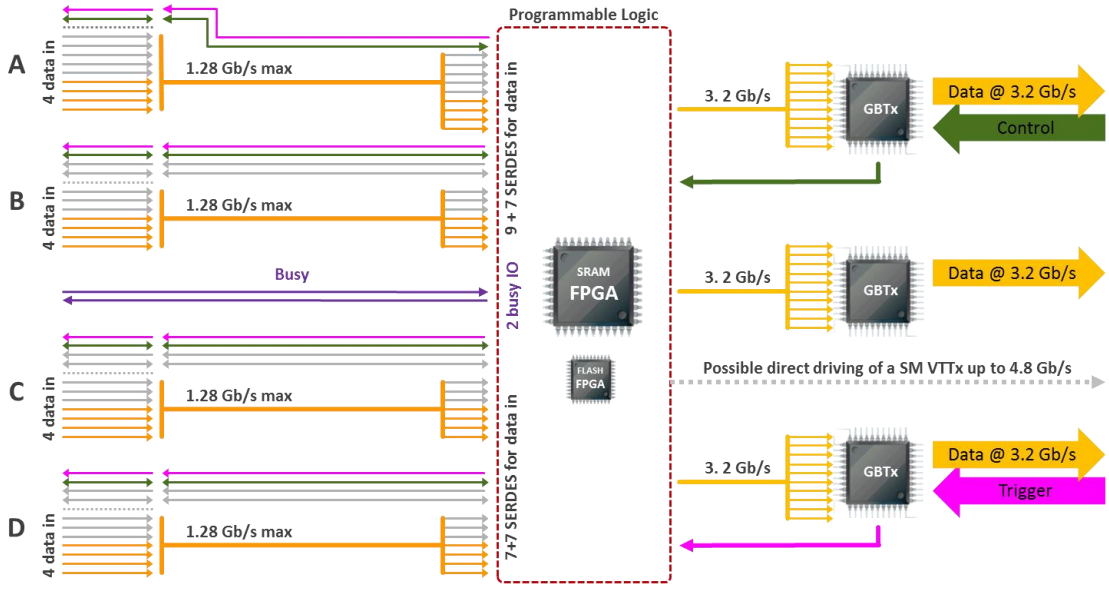

Figure 53 – **Middle Layers** data and controls routing schematic.

Figure 54 illustrates the Outer Layers connections, which is identical to the Middle Layers one scept for the number of connected data lines from the sensors.

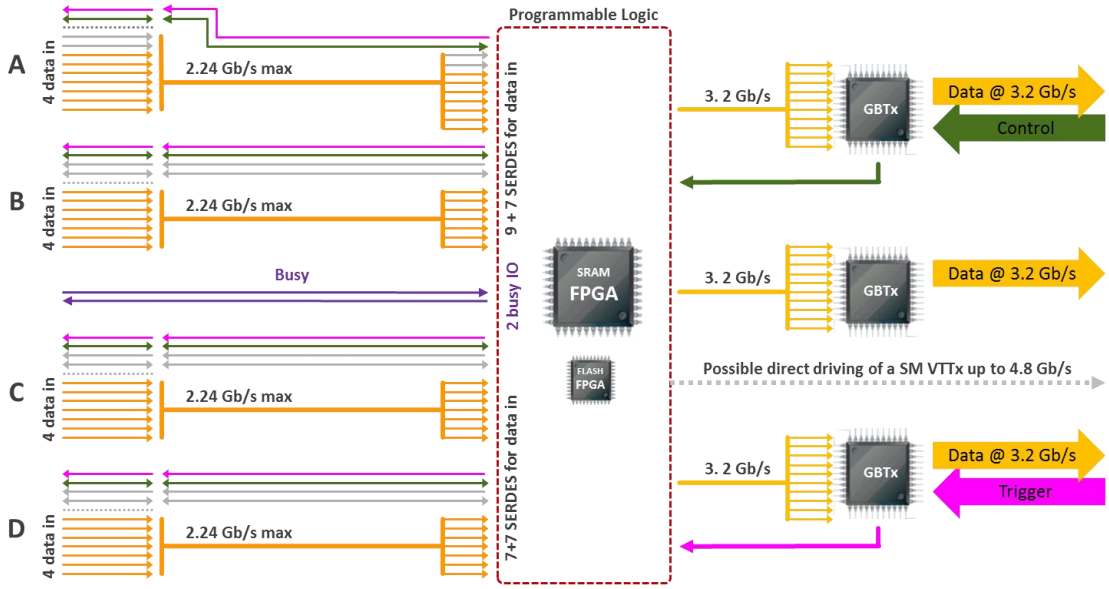

Figure 54 – **Outer Layers** data and control routing schematic.

4.2.4 Form factor

From design considerations and the first prototype test, it seems very reasonable that a Readout Unit will fit into a standard 6U VME board (233 × 160 mm^2). All the connection will stay on the front panel to make board maintenance easier, with the possible exception of the main power connection, which will depend on the chosen crate layout. The crates for the board are likely to be custom-made, with no bus or electrical facilities, again the only possible exception being a common power rail. Figure 55 illustrate a possible layout for the front of the board, with the four Firefly connectors (see 4.1.2) at the leftmost. Two further connectors for controlling the two Power Unit in the Middle and Outer Layers are on the right of the Firefly connectors (just placeholder in the figure). Three SFMP+ connectors receive the control and trigger signals, and transmit the data through three fibres. Two RSA connectors will input and output of the busy signal. The rightmost connector is the power one, which could be scrapped in favour of a backside powering connection in case is opted to go for a common power rail within the crate.

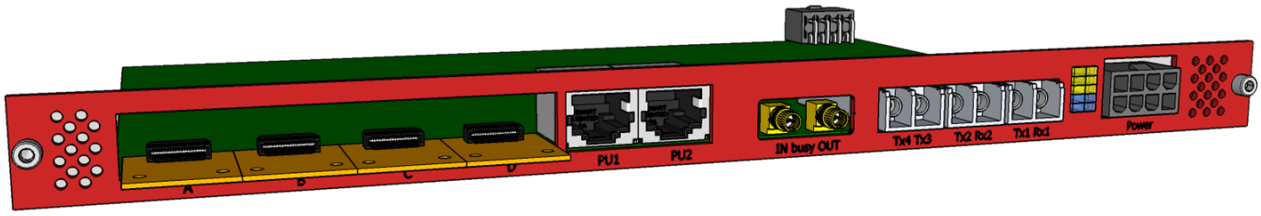

Figure 55 – Likely RU front panel in standard VME format.

4.2.5 Radiation effects

Based on the data discussed in 1.3.2 and the actual placement of the Readout Units (see 4.6), a flux of about 1 kHz of charged particle of enough energy (> 20 MeV) to generate a Single Event Effect (SEE) in the active components is foreseen. The expected low Total Ionizing Dose (< 10 krad), while it will require testing to qualify all the components, does not pose any major threat.

SRAM FPGA BRAM upset rate

One of the main concern regards the SRAM based FPGA(s) upset rate, both for the Configuration RAM (CRAM) and the Block RAM (BRAM, available memory for logic purposes). In the technology node of choice (28 nm or 20 nm), no power latch-up of commercial device has been reported during irradiation with both protons and heavy ions, even if de-capped devices did show this behaviour during heavy ion irradiation. While BRAM upset are common to both SRAM and FLASH based FPGAS, and have to treated together with all the other upset of the logic fabric, CRAM upset are specific of SRAM devices, and pose a threat to the system reliability.

A CRAM upset could in fact alter the behaviour of the device, likely stopping it or part of it. Even if modern devices provide embedded facilities (scrubbing, frame reloading, etc.) to mitigate the problem, it is likely that time to time a device will require full or partial re-programming to restore its full functionality. Based on the available data in literature, Table 24 show how frequently different upset type should occur in a Kintex 7K325 device. The total upset rate is that one derived from the CRAM cell cross-section and the over 20 MeV hadron flux. This rate does is further divided into SBU + SMBU and HMBU upset types, where:

- SBU upset are single bit upset within a CRAM frame, and the device is able to recover them without external intervention.
- SMBU are multiple bit upset which happen over more than one frame, so that each frame is affected by no more than one-bit upset. Even in this case, the device is able to restore the CRAM integrity autonomously.
- HMBU are multiple bit upset happening within the same frame, in which case it is necessary to reload the entire frame to restore it.

The reload interval column is simply a conversion in minutes of the HMBU frequency, and it provides an approximate figure of the interval between reloads of part (or the full) firmware.

Position respect to beam			Flux	Estimated CRAM upset rate			
R	Z	Reference name	High energy hadron flux*	Total	SBU + SMBU	HMBU	Reload interval
[cm]	[cm]		[kHz cm^{-2}]	[s^{-1}]	[s^{-1}]	[s^{-1}]	minutes
43	[-73.7 ÷ 73.7]	ITS L6	3.4 (4.9)	2.4×10^{-3}	2.1×10^{-3}	1.8×10^{-4}	90 (≈1h)
79	[-260 ÷ 260]	TPC In	1.35 (1.8)	8.2×10^{-4}	7.4×10^{-4}	8.2×10^{-5}	200 (≈3h)
100	**330**	**RE**	**0.86**	**4.8×10^{-4}**	**4.4×10^{-4}**	**4.8×10^{-5}**	**344 (≈6h)**
258	[-260 ÷ 260]	TPC Out	0.27 (0.37)	8.2×10^{-5}	7.4×10^{-5}	8.2×10^{-6}	1273 (≈21h)
290	[-290 ÷ 290]	TRD	0.23 (0.31)	6.3×10^{-5}	5.7×10^{-5}	6.3×10^{-6}	1495 (≈25h)

- High-energy hadrons and charged particles flux are those expected for HL-LHC.
- The average value within the z span is reported first, in brackets the peak value within the z interval.
- * Momentum > 20 MeV.

Table 24 – Estimated CRAM upset rate for a Kintex 7K325 device at different locations.

Data reported in Table 24 are a worst-case scenario, as they are assuming full utilization of the device CRAM (usually 30% or less is used for a full device) and that all HMBU CRAM upsets will affect a critical part of the design. For example data paths and buffers, which will occupy most of the resources, are not critical, and the system could operate unaffected while that particular CRAM block is being reloaded.

However, considering that the full Readout Electronic will use about 400 such or equivalent devices, the worst case scenario calls for an FPGA stopping working and requiring some intervention every about 50 seconds. This makes it clear the importance of designing the system to cope with that, and to demand vital task to different devices (FLASH FPGAs) or to fail-proof redundant layouts (e.g. design hard-partitioning within a single device).

SERDES upset rate

Power converters latch-up

4.3 Trigger distribution

The Central Trigger Processor (CTP) ships the trigger through a dedicated Versatile Link directly to the Readout Units. Since the CTP cannot source more than a few fibres, the signal will have to be duplicated. Two options are currently under investigation: full passive optical splitting and mixed electrical/optical splitting.

4.3.1 Trigger splitting

In the case of full optical splitting, a ratio of 32 to 1 would be necessary to cover the 192 RU starting from six source fibres from the CTP. Such a ratio seems difficult to achieve, but dedicated R&D is nevertheless ongoing. Alternatively, electrical splitting should happen in the very first stage, and then a less aggressive optical splitting of 16:1 or 8:1. While jitter is not a concern considering the required trigger alignment precision (50 ns or better, and anyway re-alignment is possible within the RUs), the electrical splitting will require the design and commissioning of an additional electronic board, to be somehow integrated in the CTP .

Whichever the final splitting topology, as long as optical splitting will be present (the most likely scenario), it will be necessary to use Single Mode (SM) fiberoptics components, as passive optical splitter exist for SM fibres only. Newer splitter for Multi Mode (MM) fibres did start appearing (spring 2016), but at present their cost is much higher and they are difficult to get. Therefore, a Single Mode optical chain is envisaged for distributing the trigger to the RUs, which will require specific components validation, as the VTTx and VTRx transceiver used for the data and control optical links are MM ones.

4.3.2 Trigger timing

Sensor timing considerations from 2.3.1 sets the maximum trigger latency better than 2.0 µs. Table 25 shows how using the L0 trigger leaves virtually no safety margin nor room for any trigger processing within the RU, hence the decision is to use the LM trigger, which guarantees better time margin in managing the trigger signal.

Trigger timing [ns]		
Stage	LM	L0
Input at CTP	425	1200
CTP processing	100	100
Low Latency Interface	65	65
LTU	25	25
GBT downstream latency	150	150
Optical path to RU (35m)	175	175
Link from RU to sensor	250	250
Total	1190	1965

Table 25 – Trigger timing

4.4 Power supply and control

4.4.1 DC-DC converters

4.4.2 Test Power Unit

4.5 Busy Signal

The design of the Readout Units foresees the possibility of generating a busy status signal at different levels, the experiment requirements defining which option will go in the final implementation. In the limit the timing is not critical, because the busy status of any sensor is anyway sent through the standard data path at every readout cycle, a dedicated busy management system is not necessary at all, as the global busy information can be derived at the Common Readout Unit level.

In the eventuality a "fast" (few microseconds or better) busy status information is deemed necessary, the preferred implementation uses the RUs themselves to generate stave-level busy information, and then stitch them together through the use of Local Busy Units (LBU) which then collects the data in a Master Busy Unit (MBU). In such scheme, each RU generates a bitmap of the busy status of the sensors (modules) it reads, and as soon as it is complete, it sends it out to the Busy Unit. The master Busy Unit is another Readout Unit with specific firmware (or with a specific part of the firmware enabled) which collects the different busy bitmaps and generates a global busy status, issuing flags in case specific condition are meet (e.g. more than a give percent of sensors busy, or clusters of busy sensors, etc).

In case a global busy representation is not necessary, or the timing is less critical, each RU could simply ship the Busy Bitmap to the CRU through the standard data lines. If speed is important but no global busy status is necessary, each RU could ship the busy status using one of the GBT channel not used to upstream the data, as three fibres will be available upstream, and it is unlikely (considering the sensor noise figures ad Jan 2016) that more than two of them will be necessary for data.

4.5.1 Busy representation

The busy status bitmap uses a 16 bit double word to represent the busy status of an Inner Layer stave (9 sensors) or a module (14 sensors)

4.5.2 Busy routing

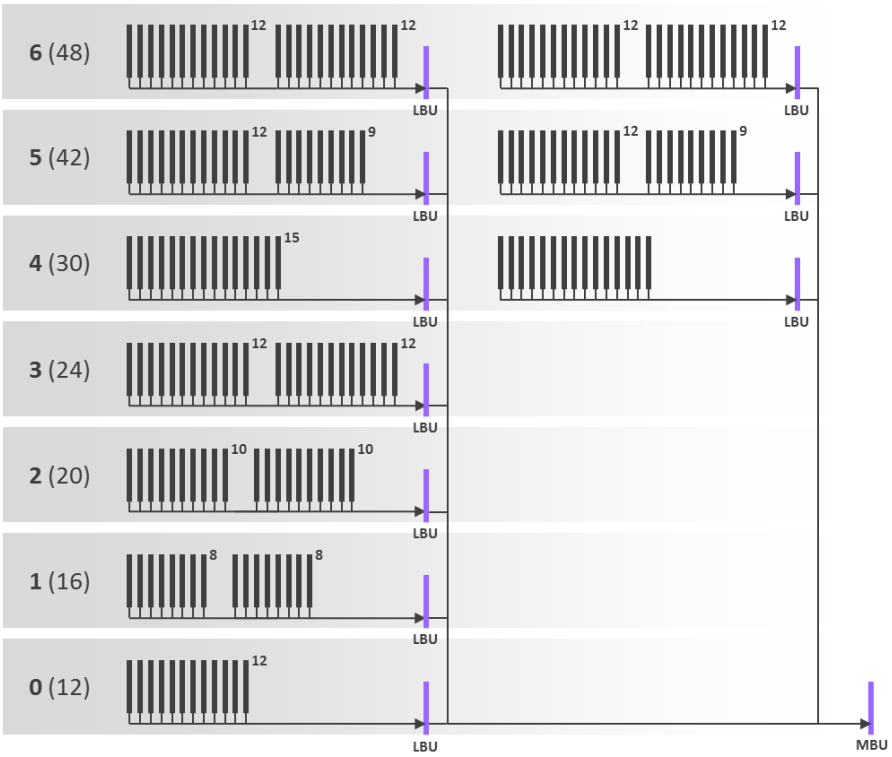

Figure 56 – Busy signal routing with local and master busy units highlighted in purple.

4.6 Layout

The 192 Readout Units must sit close enough to the end of the stave to allow the connection with 5m or shorter copper cables, to ensure the link will run at the required speed of 1.2 Gb/s. At the same time, moving away the RUs from the interaction point decreases the radiation flux, therefore decreasing the SEU rate in the electronic. Signal (trigger, busy) distribution, cooling and mechanical constraints further limit the freedom in the RUs placement.

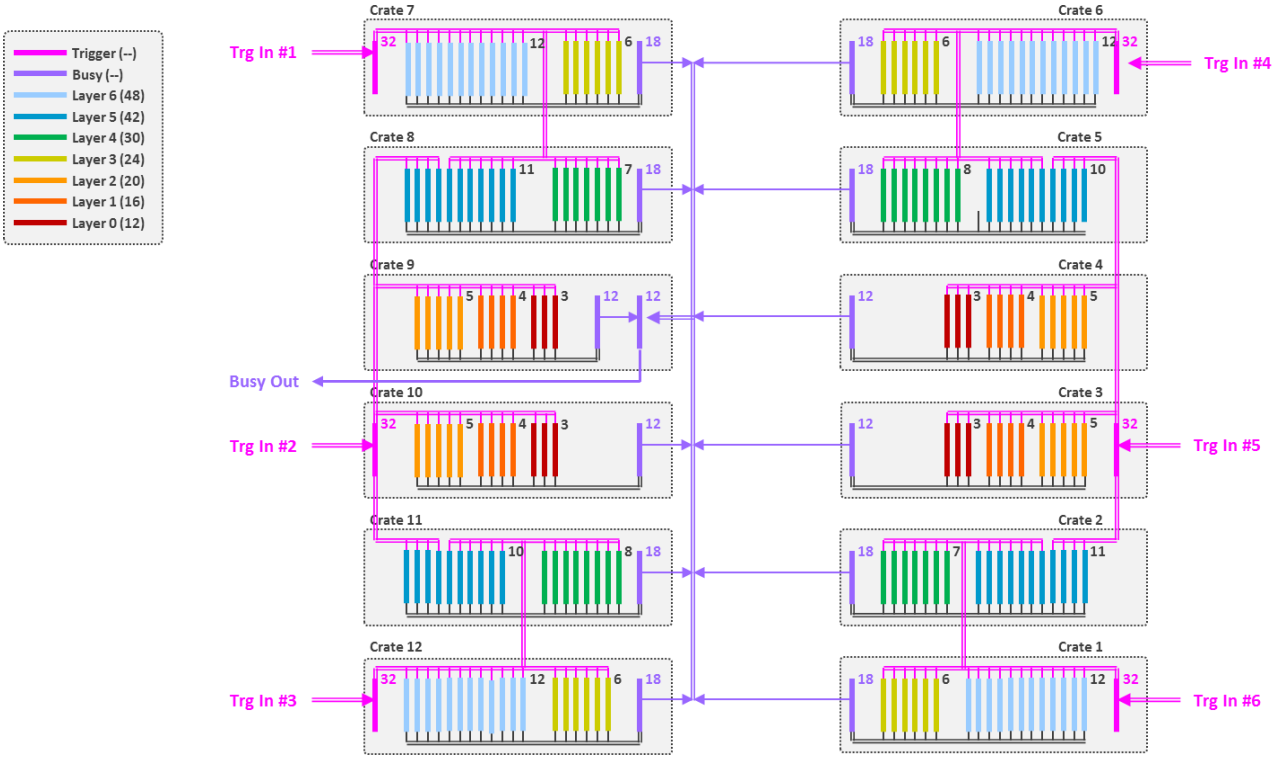

Figure 57 – RUs layout with trigger and busy possible connections.